

Hole Superconductivity xOr Hot Hydride Superconductivity

J. E. Hirsch *

Department of Physics, University of California, San Diego, La Jolla, CA 92093-0319

Under the spell of BCS-electron-phonon theory [1], during the last 6 years experimentalists have purportedly discovered a plethora of high temperature conventional superconductors among pressurized hydrides [2, 3], and theorists have been busy predicting and explaining those findings [4–6]. The alternative theory of hole superconductivity [7] predicts instead that *no superconductivity* can exist in these materials. In this Tutorial I will first argue that, unclouded by the prejudice of BCS’s validity, the existing experimental evidence for superconductivity in pressurized hydrides does not withstand scrutiny. Once it is established that superconductivity in pressurized hydrides is a myth and not a reality, the claim to validity of BCS-electron-phonon theory as a descriptor of superconductivity of real materials will be forever shattered, and an alternative theory will become imperative. I will explain the fundamentals of the theory of hole superconductivity, developed over the past 32 years [7, 8], and why it is compelling. Crucially, it explains the Meissner effect, that I argue the conventional theory does not. It applies to all superconducting materials and provides guidelines in the search for high temperature superconductors that are very different from those provided by BCS-electron-phonon theory. Light elements are predicted to be irrelevant to warm superconductivity, because according to this theory the electron-phonon interaction plays no role in superconductivity.

PACS numbers:

I. INTRODUCTION

Over the past 65 years, BCS-electron-phonon theory has been generally accepted as the correct explanation of superconductivity in conventional materials [1]. Yet before the hydride era, BCS was notoriously *unable* to predict new superconducting materials before they were experimentally discovered [9, 10]. A tectonic shift took place in 2015 when Mikhail Erements, guided by a theoretical prediction [11], discovered “Conventional superconductivity at 203 kelvin” in sulfur hydride under pressure [12]. Since then, BCS theory has been the driving force and guiding light in the search and discovery of high temperature superconducting hydrides under pressure [4–6]. The hydrides have been BCS’s greatest triumph. As the other side of the same coin, if it is eventually established that there never was superconductivity in the hydrides, this will become BCS’s greatest and final defeat. The credibility of BCS as a predictor of superconductivity in real materials will be forever shattered.

How do we *know* that conventional superconductivity exists in pressurized hydrides? The reality is, we don’t. The scientific community currently believes it does, largely because (i) the conventional BCS-electron-phonon theory of superconductivity [1] predicts that high temperature superconductivity should occur in these materials [13, 14], and (ii) the conventional theory is believed to be correct and to describe many materials in nature. Propelled by this belief, high temperature conventional superconductivity in pressurized hydrides has been intensively searched for in recent years [15, 16], and

phenomena that have been observed suggestive of superconductivity in these materials [12, 17–34] have been interpreted as proof that they are superconductors.

I share the general belief that (i) is true, as most physicists do. However, if (ii) is not true, i.e. if the conventional theory of superconductivity is not correct and does not describe real materials [36], the case for high temperature superconductivity in pressurized hydrides falls apart. If so, the detailed theoretical calculations that predict it and explain it [2, 5, 37–57] are a myth unrelated to physical reality, and the experimental observations suggesting the existence of high temperature superconductivity in pressurized hydrides [12, 17–34] have a different explanation that is *not* superconductivity.

The theory of hole superconductivity [7] predicts that *no high temperature conventional superconductivity exists in pressurized hydrides*. Or any other high temperature superconductivity for that matter. If it does exist, the theory of hole superconductivity will be proven wrong. In this Tutorial I will explain why the theory of hole superconductivity is compelling and therefore no high temperature superconducting hydrides can exist. This implies that the phenomena reported to occur in these hydrides at high pressure interpreted as indicating superconductivity are not associated with superconductivity.

Enormous research efforts and resources are being currently devoted to high temperature superconductivity in hydrides [58, 59]. If the phenomenon does not exist, those efforts and resources are wasted. They should instead be redirected to either the study of other phenomena in hydrides that are real and could lead to important technological applications for the benefit of society, or to the study of real superconductivity in systems where it really exists. For these reasons it is important to settle this question as soon as possible. This Tutorial is a con-

*Corresponding author *email*: jhirsch@ucsd.edu

tribution to that goal. I am grateful to the Editors of this Special Topics volume for the invitation to write it.

II. EVIDENCE FOR AND AGAINST HIGH TEMPERATURE SUPERCONDUCTIVITY IN PRESSURIZED HYDRIDES

Before delving into the alternative theory of hole superconductivity, to motivate the reader to do so, let us briefly discuss the existing experimental and theoretical evidence on superconductivity in pressurized hydrides.

A. Theoretical

Theory has predicted high temperature superconductivity for numerous hydride materials under high pressure. For a few of them, experimental evidence suggesting superconductivity has been found [12, 17–34]. However for a much larger number of them, no evidence of superconductivity has been found. Ashcroft originally suggested [14] compounds of hydrogen and group IV elements, methane, silane, germane, stannane and plumbane as the best candidates. No evidence for superconductivity has ever been reported for methane, germane nor plumbane. For silane, Erements has claimed superconductivity at 17K at pressure $\sim 100\text{GPa}$ [60], but the result has never been reproduced and the T_c found is substantially smaller than was predicted theoretically [61–64]. For stannane, it was predicted that it would become metallic and superconducting above 70 GPa [65] with T_c in the range 60 – 75K, some evidence for a resistance drop interpreted as superconductivity at such temperatures was recently found but at much higher pressure, 200 GPa [31] and the result has not been reproduced. Aluminum hydride was found to be metallic above 100 GPa but no superconductivity was detected down to 4K contrary to theoretical predictions [66]. Superconductivity has been predicted to exist in lithium hydrides [67], potassium hydrides [68], beryllium hydrides [69], magnesium hydrides [70], selenium hydrides [71, 72], tellurium hydrides [73], vanadium hydrides [74], niobium hydrides [75], antimony hydrides [76], arsenic hydrides [76], scandium hydrides [77], uranium hydrides [78], chromium hydrides [79], tungsten hydrides [80], zirconium hydrides [52], actinium hydrides [81], etc, but no evidence for it has been found so far.

Concerning the reliability of theoretical studies that predict superconductivity in hydrides under high pressure, it is interesting to note that recently on the very same day two theoretical studies appeared on arXiv by reputable theorists [82, 83], reporting their theoretical analysis on the possibility of room temperature superconductivity in carbonaceous sulfur hydride [29] and reaching diametrically opposed conclusions.

Finally, one may wonder: why is it that the conventional theory is assumed to be able to accurately predict

superconductivity in pressurized hydrides? Historically, the conventional theory of superconductivity has been notoriously *unable* to predict superconductivity [9, 10] in any of 32 classes of superconducting materials [84, 85] *except* pressurized hydrides [15, 84]. Why would that be? There is no argument that hydrides are ‘simpler’ than other materials. I suggest that the only reason that theory appears to be much more successful in predicting superconductivity in pressurized hydrides than in other classes of materials is simply that experimentally it is much more difficult to establish the presence or absence of superconductivity in pressurized hydrides versus in materials at ambient pressure.

B. Experimental

Experiments on hydrides under high pressure are extremely difficult to perform and interpret. Samples are very small, pressures are very high, and potentially other effects caused by the sample’s environment unrelated to the physics of the sample could give rise to signals that may be interpreted as evidence of superconductivity but are not. Because of this it is very important to guard against “confirmation bias”, the natural tendency to give high value to information that confirms prior beliefs or expectations and give low value or even discard information that does not. This is particularly important in this case because of the strong a-priori expectation that follows from the theory discussed in the previous subsection.

A clear illustration of this phenomenon is the inordinately high value given in papers on this subject to the experimental observation of an isotope effect in several of these materials [12, 19, 23, 24], interpreted as confirmation both that they are superconductors and that the mechanism is conventional. The fact is, there are many cases of materials believed to be conventional superconductors where the isotope coefficient measured is *not* $\alpha = 0.5$, as expected from BCS theory [86]. There are elements with isotope coefficient zero [86] and even negative [87]. Even more remarkable is the fact that for the “old” hydrides at ambient pressure, such as PdH with $T_c \sim 10\text{K}$, the isotope coefficient is large and negative, i.e. PdD has higher T_c than PdH [88]. This has been interpreted as due to anharmonicity [89]. It is likely that if the measured isotope coefficient in e.g. sulfur hydride had been negative, such an explanation would have been invoked. In fact, it has been proposed that anharmonicity is strong in sulfur hydride [90]. It should also be remembered that there is an isotope effect in the energy gap of *semiconductors* [91], and nobody argues that the energy gap in semiconductors is *caused* by the electron-phonon interaction. Therefore I argue that in the absence of confirmation bias the measured isotope coefficient does not provide strong evidence for nor against superconductivity.

For hydrides where some experimental evidence in-

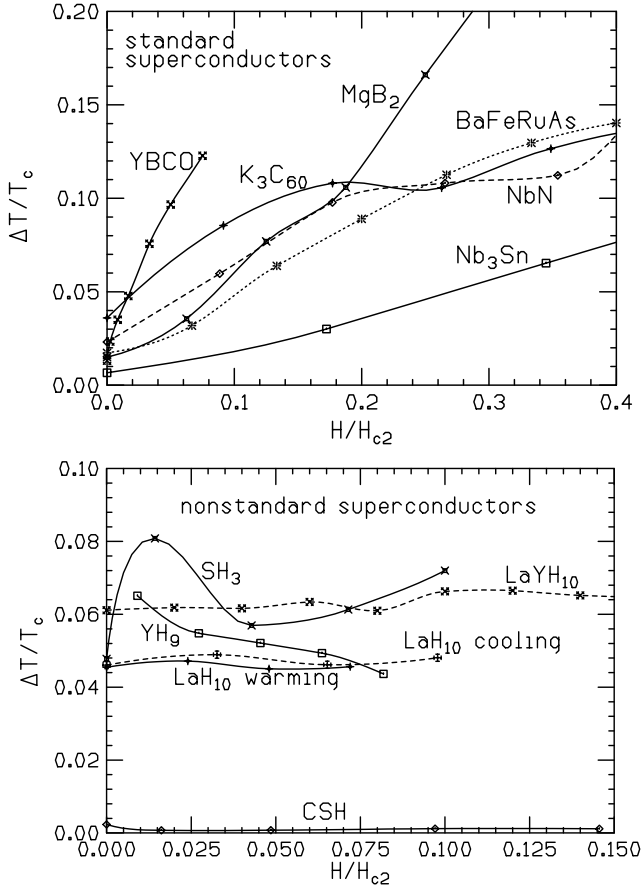


FIG. 1: Width of the resistive transition ΔT versus applied magnetic field. Contrary to standard type II superconductors (upper panel) many hydrides under pressure show no broadening of the transition with applied magnetic field (lower panel) [94].

terpreted as showing superconductivity has been found [12, 17–35], I would like to summarize here arguments against it.

1. Resistive transition

The unusual sharpness of the resistive transitions reported in some cases [29] and the absence of broadening of the resistive transition in the presence of strong magnetic fields seen in many cases [19, 24, 29], shown in Fig. 1, strongly suggest that they are not associated with superconductivity [92–94]. We have discussed theoretical reasons for why in a standard type II superconductor a broadening of the resistive transition with applied magnetic field necessarily happens [92–94]. The broadening is expected to be larger for high temperature superconductors. Instead, fig. 1 shows that in many hydride superconductors the width of the resistive transition is insensitive to applied magnetic field, even for the claimed room temperature superconductor CSH [29]. For the lat-

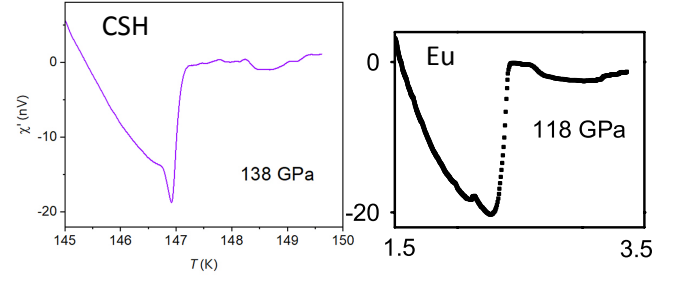


FIG. 2: Raw data for ac magnetic susceptibility of CSH [29], reproduced with permission from Nature Publishing, copyright 2021 Nature Publishing, and of Eu under pressure, reproduced from ref. [95] with the permission of AIP Publishing.

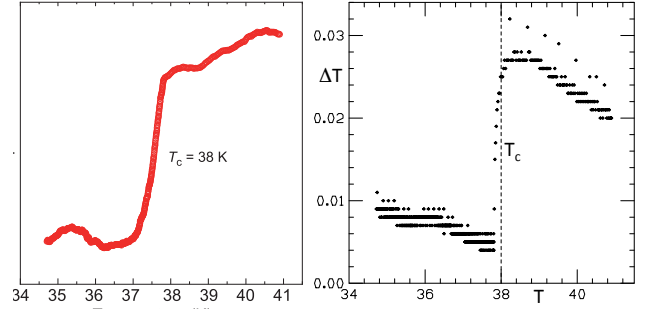


FIG. 3: Left panel: ac magnetic susceptibility of sulfur hydride, from [101], reproduced with permission from National Science Review, copyright 2019 National Science Review. Right panel: temperature interval between successive measurements in the left panel, from raw data [102]. The dashed vertical line was inserted at 38K, the assumed T_c .

ter case, the width of the transition also in the absence of magnetic field is implausibly small, as seen in Fig. 1. If in some hydrogen-rich materials under high pressure there are resistance drops as the temperature is lowered that are unrelated to superconductivity, whatever the reason is for it would presumably explain the resistance drops in all these materials.

2. Ac magnetic susceptibility

Ac magnetic susceptibility is a superior test of superconductivity. It should show a drop at the superconducting transition temperature. Instead, as the left panel of Fig. 2 shows, for the room temperature superconductor CSH [29] it shows a sharp drop followed by a steep rise at lower temperature. Remarkably, the same anomalous behavior is seen for the metal Eu, as shown in the right panel of Fig. 2 [95]. To understand what this means [96] it should be known that: (i) the same researcher performed the measurements for both cases [97]; (ii) the authors of [29] have refused to share the raw data associated with these measurements [98]; (iii) examination of the

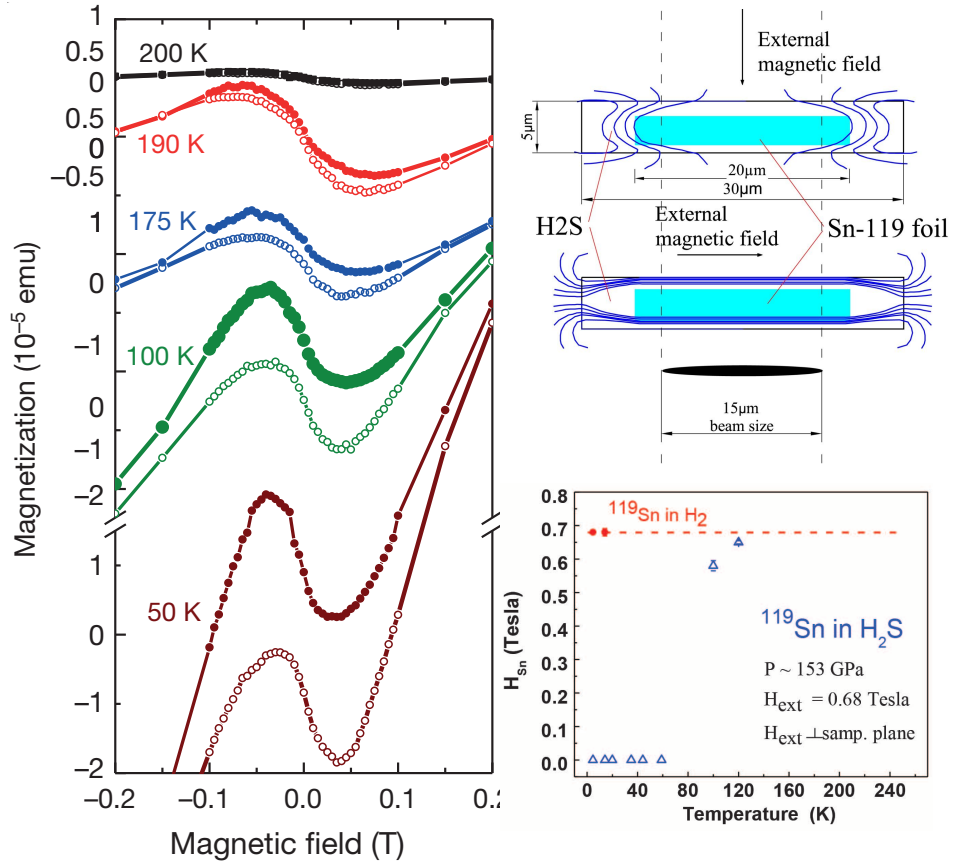


FIG. 4: Left panel: magnetization versus magnetic field for sulfur hydride, from ref. [12], reproduced with permission from Nature Publishing, copyright 2015 Nature Publishing. Right panel: alleged detection of Meissner effect in sulfur hydride using nuclear resonant scattering, from ref. [104], reproduced with permission from Science Publishing, copyright 2016 Science Publishing. The left and right panels contradict each other, see discussion in text.

raw data for ac susceptibility of Eu has shown that the published data are fraudulent [99, 100]; (iv) the published curves for ac susceptibility of CSH [29] show anomalous coincidences suggesting data manipulation [96].

For sulfur hydride, ac magnetic susceptibility measurements have been published claiming to show superconductivity in the material [101]. Fig. 3 a shows an example of the published results, from which the authors inferred a critical temperature $T_c = 38\text{K}$. The right panel shows the temperature increment ΔT between successive measurements, obtained from raw data supplied by the authors. It can be seen that a jump occurs precisely at the claimed critical temperature, which shows that the drop in susceptibility seen in the left panel is not a signal of superconductivity but an experimental artifact [102].

The only other ac susceptibility measurements published for a hydride [103], LaH_{10} , show very broad features with no clear indication of a superconducting transition.

3. Meissner effect

Ref. [104] claimed to measure the exclusion of a magnetic field of magnitude 0.68T from the interior of a flat superconducting sample of sulfur hydride using a nuclear resonant scattering (NRS) technique, and was hailed as “unequivocally confirming the existence of superconductivity” [105]. We pointed out that excluding such a large magnetic field is impossible for a type II superconductor in equilibrium [106]. If instead one assumes a non-equilibrium state sustained by pinned vortices, it implies that the material should trap a large amount of magnetic flux [107], which would easily be detectable but has never been reported. In addition, that result [104] directly contradicts magnetization measurements reported in the original sulfur hydride paper [12]. As the left panel of Fig. 4 shows, from ref. [12], an applied magnetic field as small as 0.1T was seen to penetrate the sample at 50K , as indicated by the fact that the magnetization turns upward. Instead, as seen in the right panel of Fig. 4, in the NRS experiment it was reported that no flux penetrated at 50K with a seven times larger applied magnetic field of 0.68T . It makes no sense that the same material

Li	Be	Superconductivity parameters for elements										B	C	N	O	F	Ne
...	0.026	Transition temperature in Kelvin									
...	...	Critical magnetic field in gauss (10^{-4} tesla)									
Na	Mg	...										Al	Si*	P*	S*	Cl	Ar
...	...											1.140	7	5
...	...											105
K	Ca	Sc	Ti	V	Cr*	Mn	Fe	Co	Ni	Cu	Zn	Ga	Ge*	As*	Se*	Br	Kr
...	0.39	5.38	0.875	1.091	5	0.5	7
...	100	1420	53	51
Rb	Sr	Y*	Zr	Nb	Mo	Tc	Ru	Rh	Pd	Ag	Cd	In	Sn(w)	Sb*	Te*	I	Xe
...	0.546	9.50	0.90	7.77	0.51	0.0003	0.56	3.4035	3.722	3.5	4
...	47	1980	95	1410	70	0.049	30	293	309
Cs*	Ba*	La(fcc)	Hf	Ta	W	Re	Os	Ir	Pt	Au	Hg	Tl	Pb	Bi*	Po	At	Rn
1.5	5	6.00	0.12	4.483	0.012	1.4	0.655	0.14	4.153	2.39	7.193	8
...	...	1100	...	830	1.07	198	65	19	412	171	803

FIG. 5: Superconducting critical temperature of elements at ambient pressure. In addition, Li at ambient pressure was recently found to be a superconductor, with $T_c = 0.0004K$. Li, with atomic weight 6.94, is the lightest superconducting element.

(sulfur hydride) at the same temperature (50K) would allow a magnetic field in the range 0.1-0.2T to penetrate and exclude a 0.68T magnetic field. We have pointed out other anomalies in the reported magnetic measurements of sulfur hydride [12] in ref. [108].

It should also be noted that the magnetization measurements reported in [12] have never been repeated, neither for H_3S nor for any other hydride, neither by the authors of [12] nor by anybody else. Given that the experiment required the design and construction of sophisticated equipment, a miniature non-magnetic cell made of Cu:Ti alloy working up to 200 GPa [12], the fact that it has never been used again in the ensuing 6 years is at the very least surprising. The paramagnetic signal that was measured, about which it was said in ref. [12] that “further study of the origin of this input is required”, has never been clarified.

No other magnetic evidence of superconductivity in pressurized hydrides has been presented to date (see however “Note added” at the end of this paper). We have proposed that measuring the presence or absence of trapped flux should be straightforward and definitively settle the question whether superconductivity does or does not exist in these materials [107].

4. Spectroscopic evidence

Photoemission, tunneling and optical spectroscopy are techniques widely used to confirm and provide additional information on superconductivity of materials. No photoemission nor tunneling experiments have been performed on hydrides under pressure, presumably

due to experimental constraints. One study of optical reflectivity exists, for sulfur hydride [109]. The paper reports evidence for a superconducting energy gap and for the role of phonons in causing superconductivity. However, a recent analysis of the raw data associated with this experiment indicates [110] that the conclusions drawn by the authors, which are in agreement with their theoretical expectations [111], are not supported by the measured data.

In summary: from the discussion in this section and the references provided, we conclude that both the theoretical and experimental evidence in favor of hydride superconductivity is flimsy, *provided* we are not prejudiced with the assumption that BCS is correct. With that in mind, let us proceed and consider an alternative understanding of superconductivity that predicts no superconductivity in hydrides but accounts for many observations in a wide range of other materials.

III. ELECTRON-PHONON SUPERCONDUCTIVITY VERSUS HOLE SUPERCONDUCTIVITY: MATERIALS EVIDENCE

The theory of hole superconductivity says that superconductors have to have hole carriers and that the electron-phonon interaction is irrelevant to superconductivity. The conventional theory of superconductivity says superconductivity is induced by the electron-phonon interaction and that hole carriers are irrelevant to superconductivity. What do real materials tell us?

Fig. 5 shows the critical temperature of superconducting elements at ambient pressure. Li and Be, the light-

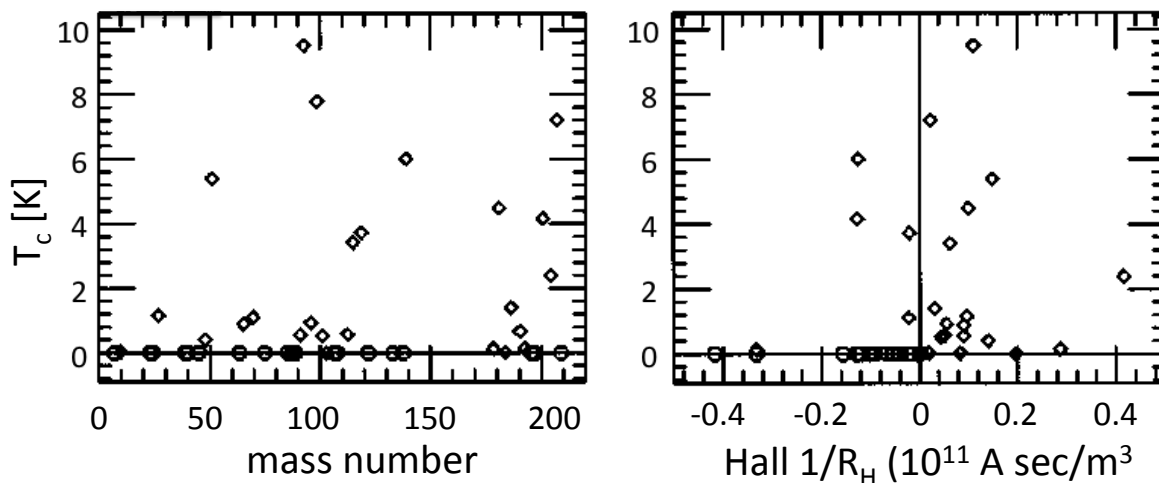


FIG. 6: Superconducting critical temperature of elements versus mass number (left panel) and versus inverse Hall coefficient (right panel).

est superconducting elements, have critical temperatures that are 20,000 and 3,000 times *smaller* than that of Pb, rather than five times *larger*, as BCS would predict. No correlation between T_c and how heavy the element is seen in Fig. 5.

Figure 6 shows the critical temperature of superconducting elements plotted versus ionic mass number (left panel) and versus inverse Hall coefficient (right panel). As expected from fig. 5, there is no indication that T_c is larger for smaller ionic mass on the left panel of Fig. 6. According to the theory of hole superconductivity, the Hall coefficient of superconductors should be positive, indicating that hole carriers dominate the transport. The right panel of Fig. 6 shows clearly that superconductivity is favored for elements with positive Hall coefficient.

The lack of correlation between ionic mass and superconducting critical temperature persists for elements under pressure. Fig. 7 shows the highest T_c 's attained by elements under pressure. There is no indication in Fig. 7 that higher T_c results from having lighter elements. For example, S under pressure has a T_c higher than Li under pressure, while being more than four times heavier. So does Y under pressure, being twelve times heavier than Li. Na and Mg, much lighter than Pb and Hg, are not superconducting with or without pressure, Pb and Hg are. La is 15 times heavier than Be while its T_c is 230 times higher rather than 4 times lower as the conventional theory would predict (everything else being equal). There is absolutely no correlation between ionic mass and superconducting T_c in the periodic table, neither under pressure nor at ambient pressure. Unfortunately, data for Hall coefficient of elements under high pressure don't exist; we have predicted that the association with positive Hall coefficient seen at ambient pressure will be even stronger at high pressures [113].

It is certainly true that the critical temperature of a BCS superconductor depends on several other properties

of the metal besides its ionic mass M , namely it increases with higher values of the density of states at the Fermi energy g and the strength of the electron-phonon coupling λ . The contribution of these however is not expected to be strongly correlated or anticorrelated with ionic mass. In other words, there is no theoretical reason for why larger M should necessarily be associated with larger g and/or larger λ , so that the decrease of T_c with larger M would be compensated by an increase of T_c with larger g or λ . In the absence of such correlation one would still expect to see a tendency towards lower T_c 's for higher M values in the periodic tables Fig. 5 and Fig. 7, superposed to fluctuations due to varying values of g and λ , however no such tendency is apparent.

There is in addition the Coulomb pseudopotential μ^* [114, 115] “wild card”, representing the effect of Coulomb repulsion within the conventional theory. It appears in the combination $(\lambda - \mu^*)$ in formulas for T_c . Because it is essentially impossible to compute μ^* from first principles, it is often used as an adjustable parameter. There is no theoretical reason to expect that μ^* should decrease with larger ionic mass, so as to counteract the expected effect of larger M in decreasing T_c .

There are of course many calculations within BCS theory that claim to reproduce the T_c 's observed in the elements. We have discussed in refs. [36, 116] reasons for why they are questionable. For example, for the simplest metal Li, superconductivity was predicted to occur at 1K [117], then the estimate was revised downward in ensuing years to explain why no superconductivity was found down to 1mK [118]. For scandium and yttrium, the fact that no superconductivity is found despite appreciable values of g and λ [120] is attributed to the effect of “spin fluctuations” [119], i.e. large μ^* . There is sufficient “superflexibility” [121] in these calculations to plausibly *postdict* any observed value of T_c .

Returning to the issue of ionic mass dependence of T_c

H	ambient pressure superconductor																high pressure superconductor										He	
Li 0.0004 14 30	Be 0.026	<div>T_c(K) T_c^{max}(K) P(GPa)</div>																<div>T_c^{max}(K) P(GPa)</div>										Ne
Na	Mg																	B 11 250	C 8.2 15.2	N 13 30	O 17.3 190	F 1.4 100	Ar					
K	Ca 25 161	Sc 19.6 106	Ti 0.39 3.35 56.0	V 5.38 16.5 120	Cr	Mn	Fe 2.1 21	Co	Ni	Cu	Zn 0.875	Ga 1.091 7 1.4	Ge 5.35 11.5	As 2.4 32	Se 8 150	Br 1.4 100	Kr											
Rb	Sr 7 50	Y 19.5 115	Zr 0.546 11 30	Nb 9.50 9.9 10	Mo 0.92	Tc 7.77	Ru 0.51	Rh .00033	Pd	Ag	Cd 0.56	In 3.404	Sn 3.722 5.3 11.3	Sb 3.9 25	Te 7.5 35	I 1.2 25	Xe											
Cs	Ba 1.3 12	insert La-Lu	Hf 0.12 8.6 62	Ta 4.483 4.5 43	W 0.012	Re 1.4	Os 0.655	Ir 0.14	Pt	Au	Hg-α 4.153	Tl 2.39	Pb 7.193	Bi 8.5 9.1	Po	At	Rn											
Fr	Ra	insert Ac-Lr	Rf	Ha																								
		La-fcc 6.00 13 15	Ce 1.7 5	Pr	Nd	Pm	Sm	Eu	Gd	Tb	Dy	Ho	Er	Tm	Yb	Lu 12.4 174												
		Ac	Th 1.368	Pa 1.4	U 0.8(β) 2.4(α) 1.2	Np	Pu	Am 0.79 2.2 6	Cm	Bk	Cf	Es	Fm	Md	No	Lr												

FIG. 7: Superconducting critical temperature of elements under pressure from ref. [112], reproduced with the permission of AIP Publishing.

in the periodic table, to minimize the incidence of varying g , λ and μ^* we can focus our attention on a given *column* in the periodic table, where elements have the same outer electron configurations and hence presumably similar electronic properties (that’s what is “periodic” about the periodic table!) including similar values of g , λ and μ^* . As we look e.g. at the variations of T_c within the columns (V, Nb, Ta) or (Zn, Cd, Hg) or (P, As, Sb, Bi) we see no indication that T_c decreases with increasing M .

Why is it that the periodic table of elements doesn’t know about “light and warm superconductors” [59]? It may have missed to read the “Dear Colleague” letter [59]. Alternatively it may be because it’s an imaginary rather than a real fact.

In ref. [122], I analyzed quantitatively how thirteen different properties of elements, including ionic mass, correlate with existence of superconductivity in the elements and with the value of T_c . I found (see Fig. 15 of [122]) that the Hall coefficient R_H has by far the largest predictive value on whether the element is ($R_H > 0$) or is not ($R_H < 0$) a superconductor, while properties associated with BCS theory such as ionic mass, specific heat (which depends on g) and electrical conductivity (which depends on λ) have essentially no predictive value [122].

The evidence that positive Hall coefficient favors superconductivity seen for the elements persists for compounds. MgB_2 , the highest T_c ‘conventional’ superconductor until the advent of the hydrides, has positive Hall

coefficient and its high T_c originates in pairing of hole carriers conducting in the B^- planes. This was predicted by the theory of hole superconductivity [123] shortly after MgB_2 was found to be superconducting [124], before its Hall coefficient was measured [125]. The conventional ‘high temperature superconductors’ before MgB_2 were the A15 materials, e.g. Nb_3Sn , Nb_3Ge , all having positive Hall coefficient [126]. Doped semiconductors that become superconducting overwhelmingly have hole carriers rather than electron carriers [127]. Soon after the high T_c cuprates were discovered it became clear [128] that holes play the dominant role in transport and give rise to their high T_c . The carriers believed to be responsible for superconductivity in electron-doped cuprates [129], initially believed to be electrons, were later established to be holes [130, 131], as had been predicted by the theory of hole superconductivity since their discovery [132].

In contrast, there is no evidence for compounds either that lighter ionic mass of the constituents favors higher T_c ’s, just like there isn’t for the elements. For example, T_c ’s of A15 compounds with V are lower than those of similar compounds with Nb , even though Nb is heavier than V . The single example suggesting that light elements would favor high T_c is MgB_2 , for which, as discussed above and in refs. [123, 133], there are good reasons that are independent of the ionic masses for why it has high T_c within the theory of hole superconductivity.

In summary: if we just consider the evidence from ma-

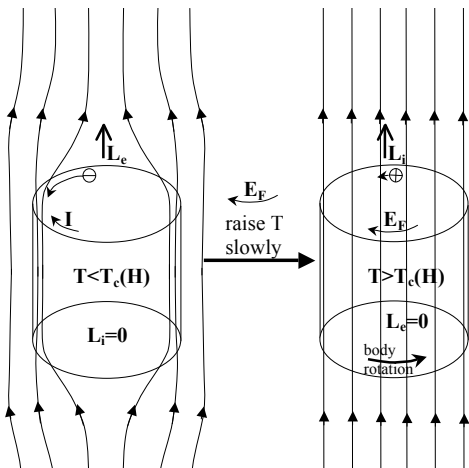


FIG. 8: A superconductor at rest in a magnetic field turns normal. The body acquires angular momentum \vec{L}_i parallel to the applied magnetic field, which equals the angular momentum \vec{L}_e initially carried by the supercurrent. The Faraday electric field E_F that develops during the process is clockwise, body rotation is counterclockwise.

materials (excluding pressurized hydrides), put aside any theoretical prejudices and ask, what is more important, the sign of the Hall coefficient or the magnitude of the ionic mass, in determining the superconductivity of a material, the answer is clearly the former. That is what the theory of hole superconductivity predicts and not what the conventional theory predicts, for which electrons or holes are indifferent.

IV. WHY HOLES ARE NECESSARY FOR SUPERCONDUCTIVITY

The fundamental reason for why holes are necessary for superconductivity is easy to explain. I will explain it below. What I cannot explain is why this is not generally known and accepted by now.

A supercurrent in a superconductor carries mechanical momentum [134]. When a supercurrent starts and stops, mechanical momentum needs to be transferred between the electrons and the body as a whole, to satisfy momentum conservation. A simply connected superconductor in a magnetic field will undergo a *reversible* phase transition as a function of temperature between superconducting and non-superconducting phases [1], where momentum needs to be transferred to and from the body as a whole *in a reversible way*.

For example, how does the supercurrent stop in going from the left to the right panel of Fig. 8, when the temperature increases and the system becomes normal? It cannot stop through onset of resistance, with the electrons transferring their momentum to the ions through collisions, since that would generate Joule heat which is an irreversible process. As pointed out by Keesom many years ago, “*it is essential that the persistent cur-*

rents have been annihilated before the material gets resistance, so that no Joule-heat is developed.” [135]. Keesom erroneously stated that the supercurrent stops by “induction” [135], but this is not so. The Faraday electric field that develops in the process of the system going normal and the supercurrent stopping is clockwise as shown in Fig. 8, while stopping the current with an electric field would require a counterclockwise field. The Faraday electric field also pushes the positive ions of the body clockwise, but the body acquires rotation in counterclockwise direction, opposing the Faraday electric field push.

Bloch [136], Heisenberg [137] and Peierls [138] just a few years earlier had found the key to answer that question: *hole carriers* in a crystalline solid transfer momentum between electrons and the body as a whole without any scattering processes that would lead to dissipation.

To understand this, figure 9 shows the forces acting on charge carriers in a Hall geometry. When the material has negative Hall coefficient ((a) above), electric and magnetic forces on *electrons* are balanced. When the material has positive Hall coefficient ((b) above), electric and magnetic forces on *holes* are balanced. Does that show a ‘symmetry’ between electrons and holes? Absolutely not.

The key is panel (c) in Fig. 9. The carriers of charge and mass are always negative electrons, holes are just a theoretical construct. Fig. 9 (c) is the same as 9 (b), redrawn showing the moving electrons. The electric and magnetic forces on the electrons are not balanced, they point in the same direction. The reason the electrons move along the current J_x is because there is another force acting on the electrons, F_l , pointing to the left in Fig. 9 (c), balancing the electric and magnetic forces. That is a force exerted by the lattice on the electrons. By Newton’s third law, the electrons in turn exert a force on the lattice F_{on-l} , pointing to the right.

Is this just a theoretical construct with no consequences? Absolutely not. The concrete physical consequence is the Ampere force \vec{F}_{Amp} , given by

$$\vec{F}_{Amp} = \frac{I}{c} \vec{L} \times \vec{H} \quad (1)$$

where I is the current, \vec{L} is a vector in the direction of I with magnitude the length of the bar, and \vec{H} is the applied magnetic field. \vec{F}_{Amp} is in the same direction, to the right in Fig. 9, whether the Hall coefficient is negative or positive. But its origin is different. In (a), it is simply $(-F_E)$, the electric force due to the Hall field acting on the positive ions. In (c) however, it is $F_{on-l} - F_E$. In the absence of F_{on-l} it would be in the wrong direction, to the left! So F_{on-l} is directly responsible for the observed Ampere force in materials with positive Hall coefficient.

F_{on-l} produces a continuous transfer of momentum from electrons to the body as a whole, that occurs without any scattering processes, through the coherent interaction of the electron wave with the periodic ionic lattice. It exists when the carriers are holes, not when they are electrons, as Fig. 9 shows. If the Hall bar in Fig. 9

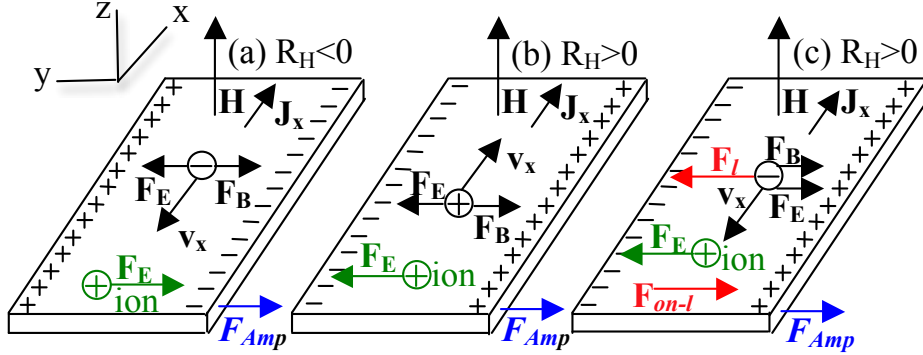


FIG. 9: Hall effect. In (a) the normal state carriers are assumed to be electrons, in (b) and (c) holes. F_E and F_B are electric and magnetic forces on the carrier, An electric force also acts on the positive ions, it is also denoted by F_E . F_l is the force exerted by the lattice on the carrier and F_{on-l} is the force exerted by the carrier on the lattice.

was free to move, it would move to the right, pushed by \vec{F}_{Amp} , acquiring momentum transferred to it by the conducting electrons. This is the principle that explains how the momentum of the supercurrent is transferred to the body as a whole when a superconductor in a magnetic field is heated and goes normal and the supercurrent stops. And it explains how in the reverse process when a normal metal is cooled into the superconducting state in the presence of a magnetic field the body acquires momentum opposite to the momentum being acquired by the normal electrons condensing and giving rise to the Meissner current.

The details of how this happens are explained in ref. [134] and will be discussed later in this Tutorial. If a material does not have hole carriers in the normal state, this reversible momentum transfer cannot happen. The material would not exhibit a Meissner effect so it would not be a superconductor.

V. HOLE CARRIERS IN A BAND

Besides being necessary to explain the Meissner effect, holes are necessary to pair and condense into the superconducting state. The Coulomb interaction between electrons in the periodic field of the ions will give rise to pairing if the carriers are holes and not if they are electrons [139–141].

Let us remember what holes are. They are the charge carriers in a band when the Fermi level is near its top, as fig. 10 shows. The effective mass of the carriers in Bloch theory is given by

$$\frac{1}{m_k^*} = \frac{1}{\hbar^2} \frac{\partial^2 \epsilon_k}{\partial k^2} \quad (2)$$

where ϵ_k is the band energy. For a band that is close to full, this effective mass will vary widely for the occupied states that span a large fraction of the Brillouin zone. Instead, for the empty states the effective mass will be approximately constant. That is one reason why we talk

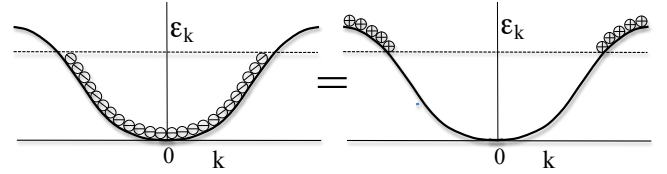


FIG. 10: When a band is close to full, we think of the charge carriers as holes, the missing electrons in the band.

about the holes and not the electrons when a band is close to full. Also, when the band is close to full, the effective mass defined by Eq. (2) for electrons is negative. That is precisely the reason for why reversible momentum transfer between electrons and the body can occur, which as discussed in the previous section is necessary for superconductivity to occur. When we talk about holes instead of electrons, we change both the sign of the charge and the effective mass, so they are both positive.

Another reason why the hole concept is useful is that the conductivity for a nearly full band is proportional to the number of holes and not to the number of electrons in the band. But we should always keep in mind that holes are not the same as particles. Most importantly, holes do not carry positive physical mass, but negative physical mass. When holes move forward, physical mass (electron mass) moves backward.

There is another fundamental reason that makes holes different from electrons that is not emphasized in textbooks. In most model Hamiltonians used to describe interacting electrons in the solid state, such as the Hubbard model, the atomic Hamiltonian is assumed unchanged under double occupancy of the orbital. The Hubbard Hamiltonian is given by

$$H = - \sum_{i,j,\sigma} [t_{ij} c_{i\sigma}^\dagger c_{j\sigma} + h.c.] + U \sum_i n_{i\uparrow} n_{i\downarrow} \quad (3)$$

where $c_{i\sigma}^\dagger$ creates an electron of spin σ in the atomic orbital at site i , with the orbital being the same whether an electron is already there or not. The doubly occupied

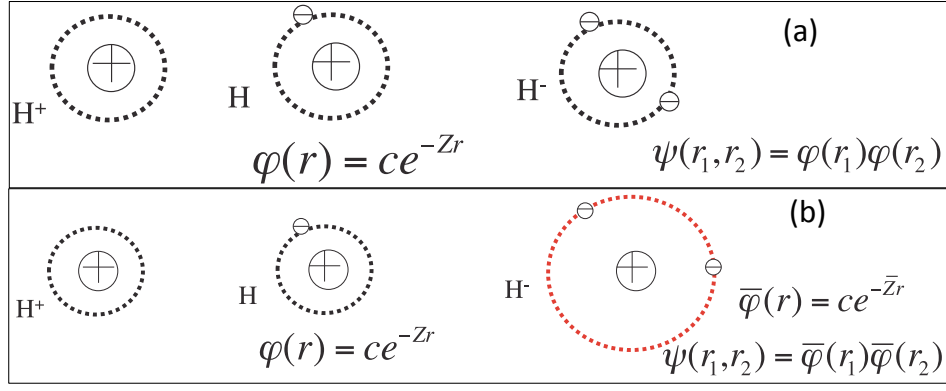


FIG. 11: The top panel shows the atomic physics assumed in most models of interacting electrons such as the Hubbard model: the atomic orbital does not change with electron occupancy. The bottom panel shows the real physics: the atomic orbital expands when it is doubly occupied.

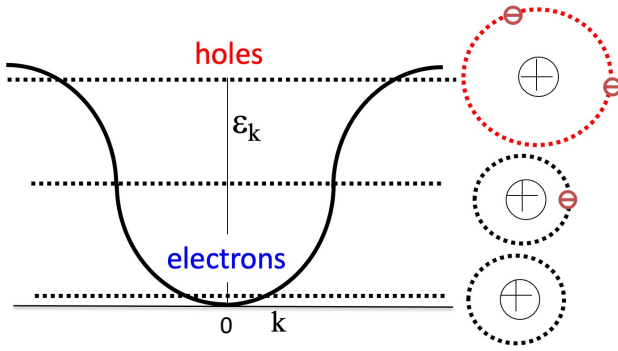


FIG. 12: Orbital expansion of doubly occupied sites will be important when the band is close to full, as shown in the picture.

atomic orbital is assumed to be a single Slater determinant, so that we have

$$|\uparrow\rangle = c_{i\uparrow}^\dagger |0\rangle \quad (4a)$$

$$|\uparrow\downarrow\rangle = c_{i\uparrow}^\dagger c_{i\downarrow}^\dagger |0\rangle \quad (4b)$$

and

$$\langle 0 | c_{i\uparrow} | \uparrow \rangle = \langle \downarrow | c_{i\uparrow} | \uparrow\downarrow \rangle = 1 \quad (4c)$$

However this is *qualitatively* incorrect, because the doubly occupied state is *never* a single Slater determinant but rather a linear combination of Slater determinants involving higher single electron states [142]:

$$|\uparrow\downarrow\rangle = \sum_{m,n} A_{mn} c_{m\uparrow}^\dagger c_{n\downarrow}^\dagger |0\rangle \quad (5a)$$

$$\sum_{m,n} |A_{mn}|^2 = 1 \quad (5b)$$

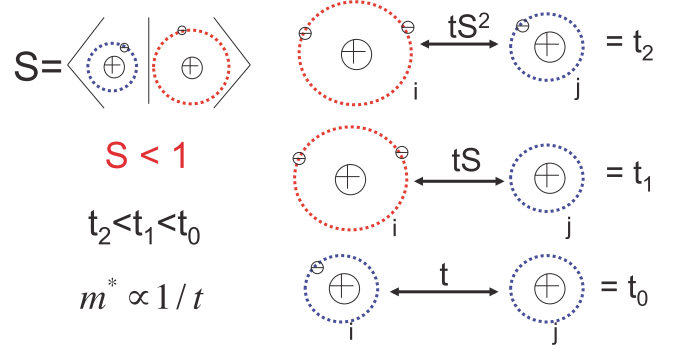


FIG. 13: The figure shows an electron hopping between two sites, with hopping amplitude that depends on how many other electrons are present at the two sites involved in the hopping process. $S < 1$ is the overlap matrix element between the expanded and unexpanded orbital.

where the sum runs over a complete set of atomic orbitals, with the lowest single particle orbital denoted by $m = 0$, i.e. $c_{0\sigma} = c_\sigma$, as well as over continuum states [143]. Eq. (5b) implies of course that $A_{mn} < 1$ for any m, n . Hence we have

$$c_\uparrow |\uparrow\downarrow\rangle = \sum_n A_{0n} c_{n\downarrow}^\dagger |0\rangle = A_{00} |\downarrow\rangle + \sum_{n \neq 0} A_{0n} c_{n\downarrow}^\dagger |0\rangle \quad (6a)$$

and

$$1 = \langle 0 | c_{i\uparrow} | \uparrow \rangle \neq \langle \downarrow | c_\uparrow | \uparrow\downarrow \rangle = A_{00} < 1 \quad (6b)$$

contrary to Eq. (4c). The inequality in Eq. (6b) reflects the basic physical fact that atoms are not electron-hole symmetric, nor are solids. The electron-electron interaction breaks particle-hole symmetry.

Because the energy difference between the atomic orbitals is smaller than U , the Hubbard electron-electron interaction, this mixing of other orbitals cannot be ignored, and the Hamiltonian Eq. (3) is qualitatively wrong [144].

To fix this fundamental flaw of the single band Hubbard model, we can use the Hartree approximation at the atomic level [145]. The main physical effect of the on-site electron-electron repulsion can be represented by an expansion of the atomic orbital when it is doubly occupied, as shown in Fig. 11. Within the Hartree approximation, the orbital with $\bar{Z} = Z - 5/16$ will minimize the energy of the doubly occupied orbital. This corresponds to an expansion of the radius of the orbital from a_0/Z , with a_0 the Bohr radius and Z the nuclear charge, to a_0/\bar{Z} . When the band is almost full, almost all the orbitals will be doubly occupied and hence expanded, as shown schematically in Fig. 12.

The expansion of orbitals upon double occupancy gives rise to a change in the hopping amplitude for electrons depending on the occupation of the sites, as shown in Fig. 13. The hopping amplitude becomes smaller as the number of electrons increases, and will be smallest when the band is almost full. Conversely, the hopping amplitude for holes will be larger if there are other holes in the sites involved in the hopping process. This gives rise to an attractive interaction between holes and to pairing and superconductivity, as discussed in the next sections.

VI. EFFECTIVE HAMILTONIAN FOR HOLE CARRIERS

The low energy effective Hamiltonian when taking into account the orbital expansion is given by [139, 146, 147]

$$H = - \sum_{ij\sigma} t_{ij}^\sigma [c_{i\sigma}^\dagger c_{j\sigma} + h.c.] + U \sum_i n_{i\uparrow} n_{i\downarrow} \quad (7a)$$

with

$$t_{ij}^\sigma = [1 + (S - 1)n_{i,-\sigma}][1 + (S - 1)n_{j,-\sigma}]t_{ij} \quad (7b)$$

with $S < 1$ the overlap matrix element between the expanded and non-expanded orbitals. Thus, the hopping amplitude for an electron between sites i and j is given by t_{ij} , St_{ij} and S^2t_{ij} depending on whether there are 0, 1 or 2 other electrons of opposite spin at the two sites involved in the hopping process. That is, the hopping amplitude becomes smaller as more electrons are added.

In terms of hole rather than electron operators, the Hamiltonian Eq. (7) becomes

$$H = - \sum_{ij\sigma} t_{ij}^\sigma [c_{i\sigma}^\dagger c_{j\sigma} + h.c.] + U \sum_i n_{i\uparrow} n_{i\downarrow} \quad (8a)$$

$$t_{ij}^\sigma = t_{ij}^h [1 + (\frac{1}{S} - 1)n_{i,-\sigma}][1 + (\frac{1}{S} - 1)n_{j,-\sigma}]t_{ij} \quad (8b)$$

with $t_{ij}^h = S^2t_{ij}$ the hopping amplitude for a single hole when there are no other holes in the two sites involved in the hopping process. The hole hopping amplitude increases as the number of holes increases, to t_{ij}^h/S and

t_{ij}^h/S^2 when there are one or two other holes at the two sites involved in the hopping process respectively. The effective bandwidth correspondingly increases. The important parameter for superconductivity is the difference in hopping amplitude for one hole in the absence of other holes, and for one hole in the presence of one other hole (of opposite spin), given by

$$\Delta t_{ij} = t_{ij}^h (\frac{1}{S} - 1) \quad (9)$$

which leads to pairing and superconductivity when the band is close to full, as discussed in the next section.

VII. PAIRING AND SUPERCONDUCTIVITY

The hopping amplitude for a hole of spin σ hopping between sites i and j is given by

$$t_{ij}^\sigma = t_{ij}^h + \Delta t_{ij}(n_{i,-\sigma} + n_{j,-\sigma}) + \Delta t_{2,ij}n_{i,-\sigma}n_{j,-\sigma} \quad (10a)$$

with Δt_{ij} given by Eq. (9) and

$$\Delta t_{2,ij} = t_{ij}^h (\frac{1}{S} - 1)^2 \quad (10b)$$

The quadratic term in electron density is unimportant for low hole density and we will ignore it in what follows. The Hamiltonian for holes is then

$$H = - \sum_{ij\sigma} [t_{ij}^h + \Delta t_{ij}(n_{i,-\sigma} + n_{j,-\sigma})][c_{i\sigma}^\dagger c_{j\sigma} + h.c.] + U \sum_i n_{i\uparrow} n_{i\downarrow}. \quad (11)$$

It can be seen that the difference in hopping amplitudes gives rise to an interaction between carriers (quartic term in fermion operators). The reduced BCS Hamiltonian is given by

$$V_{red} = \frac{1}{N} \sum_{kk'} V_{kk'} c_{k\uparrow}^\dagger c_{-k\downarrow}^\dagger c_{-k'\downarrow} c_{k'\uparrow} \quad (12)$$

with

$$V_{kk'} = 2\alpha(\epsilon_k + \epsilon_{k'}) + U \quad (13)$$

and $\alpha = \Delta t_{ij}/t_{ij}^h = (1/S - 1) > 0$. ϵ_k is the band energy

$$\epsilon_k = -\frac{1}{N} \sum_{i,j} t_{ij}^h e^{i\vec{k} \cdot (\vec{R}_i - \vec{R}_j)}. \quad (14)$$

It can be seen from Eq. (13) that the interaction is most attractive near the bottom of the band, where ϵ_k is negative (note that ϵ_k defined by Eq. (14) is zero on average). Since the Hamiltonian Eq. (11) is in hole representation, it means the interaction is most attractive for the band close to full.

The BCS gap equation

$$\Delta_k = -\frac{1}{N} \sum_{k'} \Delta_{k'} \frac{1 - 2f(E_{k'})}{2E_{k'}} \quad (15)$$

has solutions for plausible parameters for low hole concentration [139, 146]. An example of critical temperature versus hole concentration is given in Fig. 14. The BCS quasiparticle energy is given by

$$E_k = \sqrt{(\epsilon_k - \mu)^2 + \Delta_k^2} \quad (16)$$

with

$$\Delta_k = \Delta_m \left(\frac{-\epsilon_k}{D/2} + c \right) \equiv \Delta(\epsilon_k) \quad (17)$$

where D is the bandwidth, μ the chemical potential and the parameters Δ_m and c are determined from solution of the BCS equations. Figure 15 shows schematically Δ_k and E_k versus band energy. We note that Eq. (16) can be rewritten as [148]

$$E_k = \sqrt{a^2(\epsilon_k - \mu - \nu)^2 + \Delta_0^2} \quad (18)$$

with

$$a = \left(1 + \left(\frac{\Delta_m}{D/2} \right)^2 \right)^{1/2} \quad (19a)$$

$$\Delta_0 = \frac{\Delta(\mu)}{a} \quad (19b)$$

$$\nu = \frac{1}{a} \frac{\Delta_m}{D/2} \Delta_0 \quad (19c)$$

Note in Fig. 15 that because the gap function has a finite slope the minimum quasiparticle energy is shifted from the chemical potential by an amount given by ν . This reflects the essential electron-hole asymmetry of the model. Thermally excited quasiparticles here are on average positively charged [149], unlike in the standard BCS model where quasiparticles are neutral on average, half electron and half hole [1]. The net quasiparticle charge per site is

$$Q^* = \frac{2|e|}{N} \sum_k (u_k^2 - v_k^2) f(E_k) = \frac{4\nu}{Da} \int_{\Delta_0}^{\infty} dE \frac{f(E)}{\sqrt{E^2 - \Delta_0^2}} \quad (20)$$

where u_k, v_k are the usual BCS coherence factors [1] and e is the electron charge. As a consequence of this charge asymmetry, the condensate here has excess negative charge.

The pairing interaction leading to superconductivity, Eq. (9), is larger the smaller S is, the overlap matrix element between expanded and unexpanded orbitals. S is a decreasing function of Z [145], where Z represents the ionic charge of the doubly ionized atom. Therefore, the

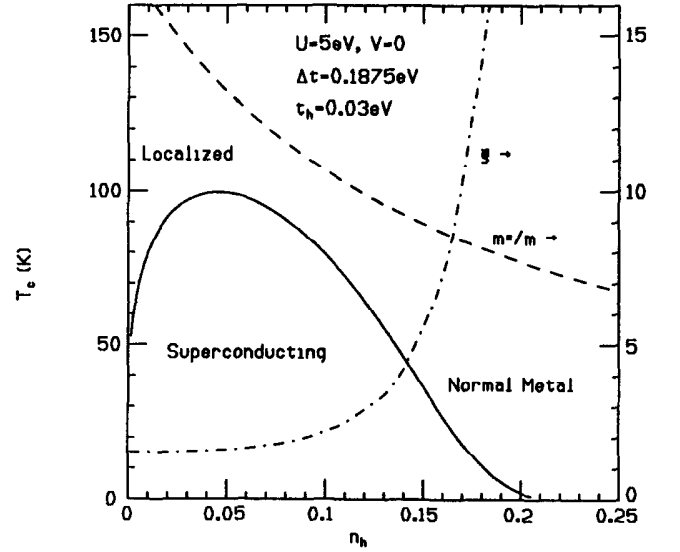


FIG. 14: Critical temperature versus hole concentration for a two-dimensional square lattice with nearest neighbor hopping only. Parameters used are shown in the figure. The figure also shows the superconducting coherence length ξ and the normal carrier effective mass versus hole concentration.

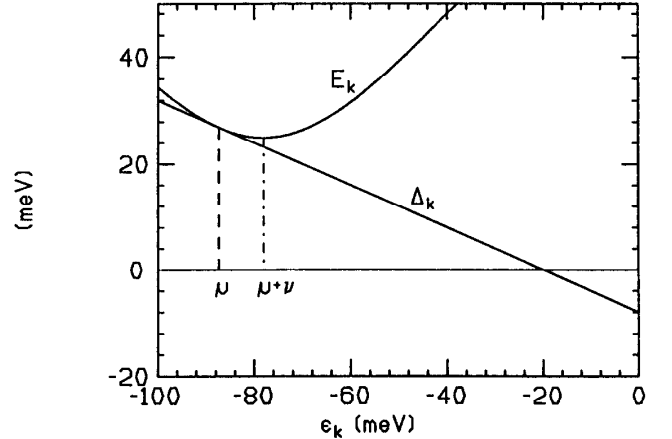


FIG. 15: Gap function Δ_k and quasiparticle energy E_k versus hole band energy ϵ_k . Parameters are: $D = 200\text{meV}$, gap slope $\Delta_m/(D/2) = 0.4$, $c = -0.2$, $\Delta_0 = 25\text{meV}$. Only the lower half of the hole band (upper half of the electron band) is shown. Note that the minimum in the quasiparticle energy is shifted from the chemical potential.

pairing interaction is larger for smaller Z and high temperature superconductivity will be favored when we have highly negatively charged atoms, i.e. anions, through which conduction through holes occurs. That is precisely the situation in the high T_c cuprate superconductors, in the superconducting pnictides and selenides, and in MgB_2 . It is not expected to be the situation in the hydrides under pressure.

Incidentally, the pairing mechanism discussed here naturally gives rise to a positive isotope effect [123]. The

parameter that drives superconductivity, Δt_{ij} , varies strongly with the distance between atoms i and j . Calling their coordinates q_i and q_j (assumed scalar for simplicity) we have

$$\Delta t_{ij} = \Delta t_{ij}^0 + \gamma(q_i - q_j) \quad (21)$$

with γ a constant related to the electron-phonon coupling [123]. The zero-point motion of the atoms will yield a small increase in the effective Δt that depends on the ionic mass:

$$\Delta t_{ij}^{eff} = \sqrt{(\Delta t_{ij})^2} = \Delta t_{ij}^0 + \frac{\gamma^2}{2\Delta t_{ij}^0} \langle (q_i - q_j)^2 \rangle \quad (22)$$

and with $\langle (q_i - q_j)^2 \rangle \sim \hbar\omega/2K$, with ω a phonon frequency and K a force constant. Thus, lighter mass gives rise to larger ω and stronger Δt_{ij}^{eff} . This can plausibly explain values of isotope coefficient observed [123].

It follows from Fig. 15 that the superconductor is characterized by having two different ‘chemical potentials’. The chemical potential μ corresponds to the condensate, and $\mu' = \mu + \nu$ to the quasiparticle excitations. In a hole representation, $\mu' > \mu$. In an electron representation, $\mu > \mu'$. The pairs forming the condensate also have a smaller effective mass than the normal state carriers, since the hopping amplitude increases from t to $t + \Delta t$ upon pairing. The negatively charged condensate, by virtue of being a superfluid as well as because of its smaller effective mass is highly mobile, in contrast to the quasiparticles which experience normal scattering and have the higher effective mass characteristic of the normal state carriers. As a consequence, the condensate will have a tendency to move out of the bulk of the superconductor, so as to tend to equate the chemical potentials μ and μ' in the bulk [150]. Because of overall charge neutrality, the negative charge will accumulate near the surface of the superconductor, giving rise to the qualitative charge distribution shown in Fig. 16. It looks like a ‘giant atom’ [151].

We can also understand this charge expulsion from the fact that thermally excited quasiparticles are on average positively charged, as given by Eq. 20. This implies that the condensate has excess negative charge, which is not fully neutralized by the positive ionic background that neutralizes the total electronic charge (condensate plus quasiparticles). The condensate is lighter than both the positive ions and the positive normal quasiparticles, so quantum mechanics dictates that its wavefunction should expand and excess negative charge should move to the surface, just like in the hydrogen atom where the light negative electron is not confined to the small spatial region occupied by the heavy positive proton. At finite temperature, to preserve local charge neutrality both the condensate distribution and the quasiparticle distribution will be inhomogeneous. At zero temperature, with no quasiparticles present, the overall charge distribution will be inhomogeneous as shown in Fig. 16.

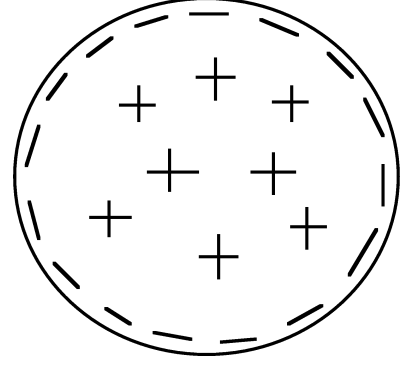


FIG. 16: Schematic picture of a spherical superconducting body. Negative charge is expelled from the bulk to the surface.

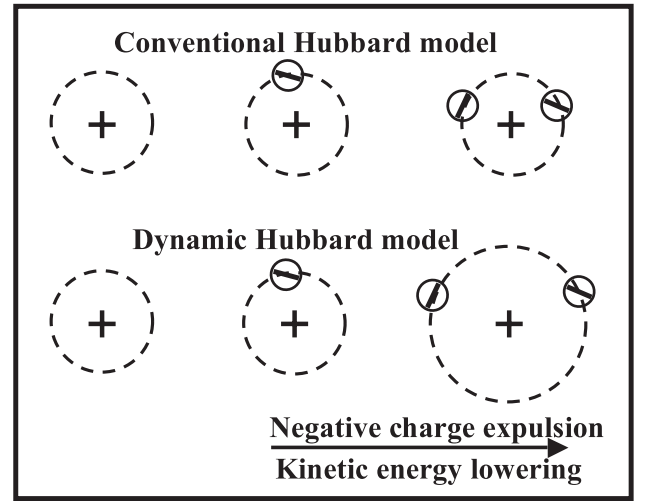


FIG. 17: For a single atom, double occupancy (pairing) causes expansion of the orbital, i.e. negative charge expulsion, and lowering of electronic kinetic energy. The same is true for the system as a whole.

VIII. CHARGE EXPULSION

The tendency of the system to expel negative charge originates in the microscopic Hamiltonian Eq. (11). At the atomic level, the atom ‘expels’ negative charge when the orbital is doubly occupied, as shown in Fig. 17. The kinetic energy of the electron is given by $\hbar^2/2m_e r^2$, with m_e the electron mass and r the orbit radius, so it is lowered when the orbit expands. As discussed earlier, the expansion gives rise to the term Δt in the Hamiltonian that breaks electron-hole symmetry.

At the level of the entire system, it is clear from the form of the Hamiltonian Eq. (11) that the kinetic energy decreases when the number of holes in the band increases, since the hopping amplitudes, Eq. (8b), increase with hole occupation. This indicates that the system will have a tendency to expel electrons from its interior to the surface, because the coordination of sites in the interior

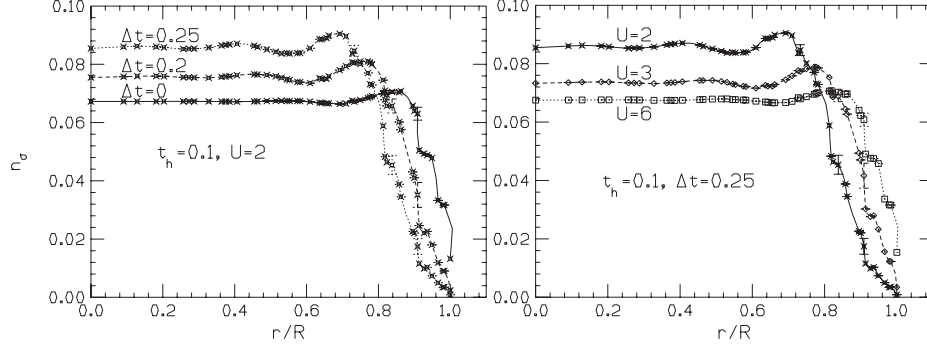


FIG. 18: Hole site occupation for various cases. As Δt increases or/and the on-site repulsion U decreases, more electrons are expelled to the surface.

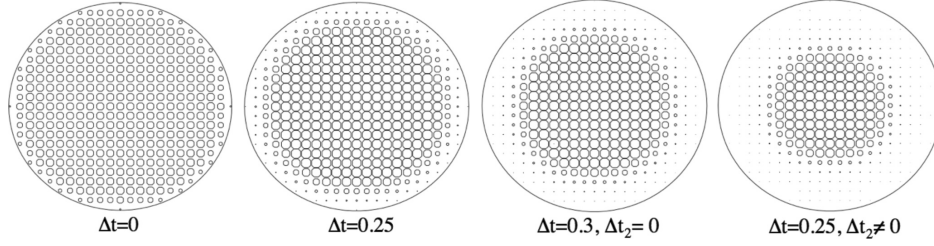


FIG. 19: The diameters of the circles are proportional to the hole occupation of the site. As Δt increases, the hole occupation increases in the interior and is depleted near the surface.

is greater than that of sites at the surface, and that will lower the kinetic energy.

This effect can be seen quantitatively within a mean field approximation [152]. We assume a cylindrical geometry of radius R and infinite length in the z direction. Decoupling the interaction terms with $\langle n_{i\sigma} \rangle = n_i/2$ with n_i the hole occupation at site i yields the mean field Hamiltonian

$$H_{mf} = H_{mf,kin} + H_{mf,pot} + H_\mu \quad (23a)$$

$$H_{mf,kin} = - \sum_{\langle ij \rangle, \sigma} [t_h + \Delta t n_i + \Delta t_2 \frac{n_i^2}{4}] [c_{i\sigma}^\dagger c_{j\sigma} + h.c.] \quad (23b)$$

$$H_{mf,pot} = \frac{U}{4} \sum_i n_i^2 \quad (23c)$$

$$H_\mu = - \sum_{\langle ij \rangle} n_i [\Delta t + \frac{n_j}{2} \Delta t_2] \sum_\sigma \langle c_{i\sigma}^\dagger c_{j\sigma} \rangle \quad (23d)$$

Note that the local average bond occupation modifies the local chemical potential. Assuming a band filling of n holes per site, we diagonalize the Hamiltonian Eq. (23) with initial values $n_i = n$ and fill the lowest energy levels until the occupation n is achieved. From the Slater

determinant of that state we obtain new values of n_i for each site and for the local bond occupation, and iterate this procedure until self-consistently is achieved. We can extend this procedure to finite temperatures, iterating to self-consistency for a given chemical potential μ . The resulting occupation of the sites as function of the distance r to the center of the cylinder is shown in Fig. 18 for various parameters. Fig. 19 shows in a diagram the hole occupation for various parameters. Larger hole occupation means smaller electron occupation

The charge expulsion tendency is largest when the parameter Δt is largest, which in turn corresponds to smaller S , the overlap of the atomic orbitals when one and two electrons are at the orbital. As discussed earlier, S is smaller when the ionic charge Z is smaller, corresponding to a more negatively charged ion. The fact that the effective Hamiltonian derived from this physics expels more negative charge the more negatively charged the ion is makes sense and can be regarded as an internal consistency check on the validity of the model.

More generally, this physics also gives rise to an increased tendency to charge inhomogeneity. Charge inhomogeneity costs potential (Coulomb) energy, so in order for it to happen it must be driven by lowering of kinetic energy. Quantitative examples are shown in ref. [152].

In the normal state, macroscopic charge expulsion as shown in Fig. 19 will not occur, it will be counteracted by longer range Coulomb repulsion in the metallic state. There cannot be an electric field in the interior of a metal. However in the superconducting state that constraint no

longer exists, there is no a priori reason why a superconductor cannot have an electric field in its interior. This is discussed in the next section.

The average quasiparticle charge as a function of position in the sample in the superconducting state can be obtained from extension of Eq. (20) to

$$Q_i^* = \frac{2|e|}{N} \sum_k (u_{ni}^2 - v_{ni}^2) f(E_k) \quad (24)$$

where the coherence factors u_{ni}, v_{ni} are now position dependent and are obtained using the Bogoliubov - de Gennes formalism [153]. An example is shown in fig. 20. The positive charge density is positive everywhere and largest near the surface, as expected.

IX. ALTERNATIVE ELECTRODYNAMICS OF SUPERCONDUCTORS

It was presciently argued by Fritz London [154] that “*It is not necessarily a configuration close to the minimum of the potential energy which is the most advantageous one for the energy balance, since by virtue of the uncertainty relation the kinetic energy also comes into play. If the resultant forces are sufficiently weak and act between sufficiently light particles, then the structure possessing the smallest total energy would be characterized by a good economy of the kinetic energy.*”

In fact, in the theory discussed here it is the lowering of kinetic energy that drives superconductivity [155], and, by pairing the charge carriers lower their effective mass [156]. A uniform charge distribution minimizes potential energy, but instead to minimize potential plus kinetic energy it is advantageous to have a non-homogeneous charge distribution, with negative charge expelled outward, just like in the atom.

The London electrodynamic theory of superconductors [154] is very naturally modified to allow for a non-homogeneous charge distribution and an electric field in

the interior of the superconductor. In fact the London brothers themselves proposed a closely related formalism in their first papers on the subject [157, 158], however later they discarded that approach in favor of what is generally accepted today [154]. Here we summarize the equations, discussed in detail in refs. [159, 160].

Starting with the London equation for the supercurrent

$$\vec{J} = -\frac{n_s e^2}{m_e c} \vec{A} \quad (25)$$

with \vec{A} the magnetic vector potential, we assume that \vec{A} satisfies the Lorenz gauge condition

$$\vec{\nabla} \cdot \vec{A} + \frac{1}{c} \frac{\partial \phi}{\partial t} = 0 \quad (26)$$

with ϕ the electric potential. The electric field is then given by

$$\vec{E} = -\vec{\nabla} \phi - \frac{1}{c} \frac{\partial \vec{A}}{\partial t} \quad (27)$$

Using the continuity equation

$$\vec{\nabla} \cdot \vec{J} = -\frac{\partial \rho}{\partial t} \quad (28)$$

and applying the divergence operator to both sides of Eq. (13) and using the gauge condition Eq. (14) yields

$$\frac{\partial \phi}{\partial t} = -\frac{m_e c^2}{n_s e^2} \frac{\partial \rho}{\partial t} \quad (29)$$

hence

$$\phi(\vec{r}, t) = -\frac{m_e c^2}{n_s e^2} \rho(\vec{r}, t) + \phi_0(\vec{r}) \quad (30)$$

$\phi_0(r)$ originates from the uniform charge density ρ_0 deep in the interior of the superconductor resulting from charge expulsion as discussed in the previous section. The charge density, electric field and electric potential then satisfy the relations

$$\rho(r) = \rho_0 + \lambda_L^2 \nabla^2 \rho(r) \quad (31a)$$

$$\vec{E}(r) = \vec{E}_0(r) + \lambda_L^2 \nabla^2 \vec{E}(r) \quad (31b)$$

$$\phi(\vec{r}) = -4\pi \lambda_L^2 \rho(\vec{r}) + \phi_0(\vec{r}) \quad (31c)$$

with $\vec{E}_0(\vec{r}) = -\vec{\nabla} \phi_0(\vec{r})$ and $\vec{\nabla} \cdot \vec{E}_0(\vec{r}) = 4\pi \rho_0$. The potential obeys

$$\phi(\vec{r}) = \phi_0(\vec{r}) + \lambda_L^2 \nabla^2 \phi(\vec{r}) \quad (31d)$$

$$\nabla^2 \phi_0(\vec{r}) = -4\pi \rho_0 \quad (31e)$$

ρ_0 a positive number determined by the microscopic parameters of the superconductor as well as the geometry,

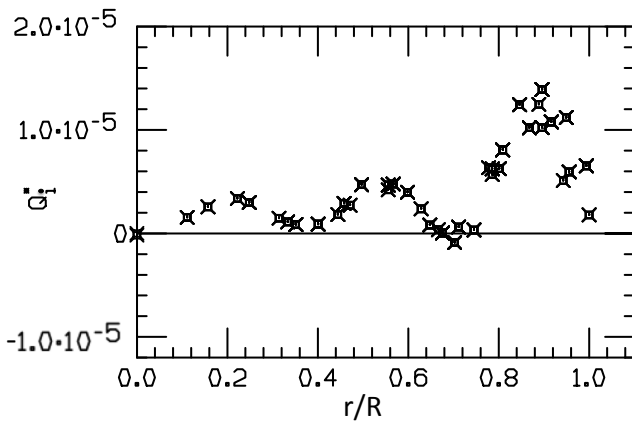


FIG. 20: Average quasiparticle charge from Eq. (24) as function of distance to the center of the sample.

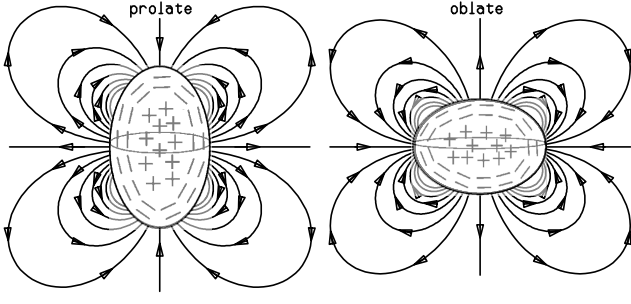


FIG. 21: Electric field line configurations for a prolate and an oblate ellipsoid, with equatorial radius a and polar radius b . Left panel: $b/a = 1.5$, right panel $a/b = 1.5$. $\lambda_L = 0.2$, $a^2b = 1.5$.

we will discuss its value later. The potential $\phi_0(\vec{r})$ is given by

$$\phi_0(\vec{r}) = \int_V d^3r' \frac{\rho_0}{|\vec{r} - \vec{r}'|}. \quad (32)$$

The electrodynamic equations can be written in relativistically covariant form as

$$\square^2(J - J_0) = \frac{1}{\lambda_L^2}(J - J_0) \quad (33a)$$

and Eqs. (40a,b)

$$\square^2(F - F_0) = \frac{1}{\lambda_L^2}(F - F_0) \quad (33b)$$

where $\square^2 = \nabla^2 - (1/c^2)(\partial^2/\partial t^2)$ is the d'Alembertian operator. F is the usual electromagnetic field tensor and F_0 is the field tensor with entries \vec{E}_0 and 0 for \vec{E} and \vec{B} respectively when expressed in the reference frame at rest with respect to the ions. In that reference frame

$$J_0 = (0, ic\rho_0) \quad (34a)$$

$$A_0 = (0, i\phi_0(\vec{r})). \quad (34b)$$

For a spherical body there is an outward pointing electric field in the interior but not field in the exterior. For other shapes, electric field lines leak out outside the body. Fig. 21 shows field line configurations for ellipsoids of revolution [161]. Electric field lines go out of regions of smaller curvature and come back in regions of higher curvature.

Note that the existence of an electric field in the interior of the superconductor neither imply a time variation of the current, as one would expect in a 'perfect conductor', nor even the *existence* of a current as in an ordinary metal. Taking the time derivative of Eq. (25) and using equation (26) yields

$$\frac{\partial \vec{J}}{\partial t} = \frac{n_s e^2}{m}(\vec{\nabla} \phi + \vec{E}) \quad (35)$$

so that in a stationary situation there can be an electric field that is derivable from a potential ($\vec{E} = -\vec{\nabla} \phi$) and it does not lead to a time-varying supercurrent. Whether a stationary supercurrent exists or not depends on the magnetic vector potential \vec{A} and not on the electric field.

X. SPIN CURRENT

The equations given in the previous section for the charge distribution of the condensate and resulting electric field acquire a deeper meaning when considering the spin degrees of freedom of the superfluid carriers. We will not get into the details here, and refer the reader to ref. [162, 163]. The expelled negative charge acquires azimuthal velocity near the surface due to the spin-orbit interaction, and circulates with velocity given by

$$\vec{v}_\sigma^0 = -\frac{\hbar}{4m_e \lambda_L} \vec{\sigma} \times \hat{n} \quad (36)$$

where \hat{n} is the normal unit vector pointing *out* of the surface. The spin current velocity as a function of position \vec{r} is

$$\vec{v}_\sigma(\vec{r}) = \frac{v_\sigma^0}{E_m} \vec{\sigma} \times (\vec{E}(\vec{r}) - \vec{E}_0(\vec{r})). \quad (37)$$

It is shown schematically in fig. 22. The excess negative charge density resides within a London penetration depth λ_L of the surface and has the simple form

$$\rho_- = n_s e \frac{v_\sigma^0}{c} \quad (38)$$

and the magnitude of the interior charge density ρ_0 is determined from ρ_- by charge neutrality and the geometry of the sample. For example a sphere of radius R , $\rho_0 = -(3\lambda_L/R)\rho_-$. The maximum electric field in the interior near the surface is given by

$$E_m = -\frac{\hbar c}{4e\lambda_L^2} \quad (39)$$

and v_σ^0 satisfies

$$v_\sigma^0 = \frac{e}{m_e c} \lambda_L E_m \quad (40a)$$

$$\frac{1}{2} m_e (v_\sigma^0)^2 n_s = \frac{E_m^2}{8\pi}. \quad (40b)$$

Electrons in the condensate reside in mesoscopic orbits of radius $2\lambda_L$. The orbital angular momentum of electrons in these orbits is [162–164]

$$\ell = m_e v_\sigma^0 (2\lambda_L) = \frac{\hbar}{2}. \quad (41)$$

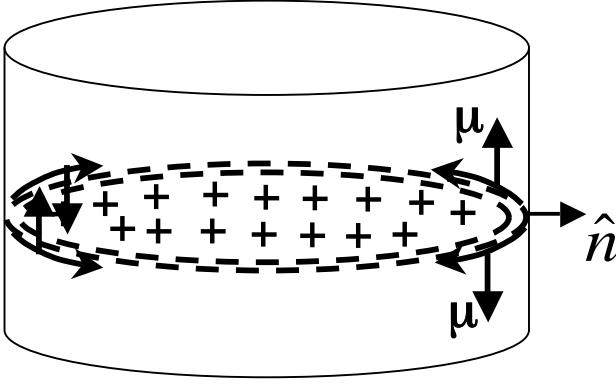


FIG. 22: Charge distribution and spin current in a cross section of a cylindrical sample. At the surface, the velocity is given by Eq. (36). The electron intrinsic magnetic moment $\vec{m}\vec{u}$ is shown in the direction indicated by the vertical arrows.

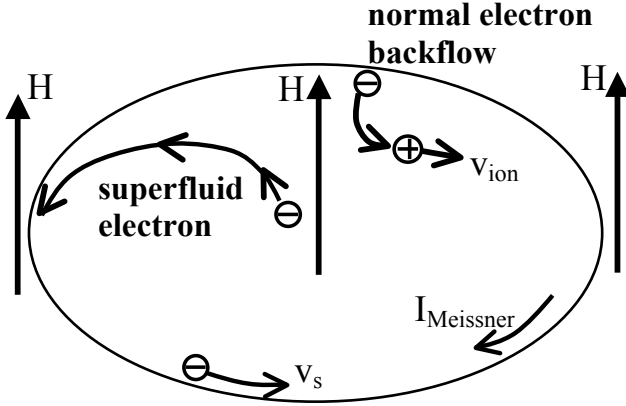


FIG. 23: The essence of the Meissner effect. Electrons becoming superfluid flow from the interior towards the surface and are deflected to the left by the magnetic field pointing up, creating the Meissner current. Normal electrons backflow from the surface towards the interior and are deflected to the right by the magnetic field. Their momentum is transferred to the ions, so the body rotates clockwise.

XI. MEISSNER EFFECT AND ROTATING SUPERCONDUCTORS

The physics of the Meissner effect, the expulsion of magnetic field from the interior of a metal becoming superconducting, is easy to understand within the theory of hole superconductivity. It is impossible to understand within the conventional theory of superconductivity.

The essential physics is shown in Fig. 23 [165]. Electrons becoming superconducting flow *outward* and acquire the momentum of the Meissner current through the Lorentz force exerted by the magnetic field \vec{H} . Normal backflowing electrons acquire azimuthal momentum in opposite direction also through the Lorentz force, and transfer that momentum to the lattice.

In more detail the process is shown in Fig. 24 [134].

The phase boundary is moving outward. Electrons at the boundary becoming superconducting expand their orbits to radius $2\lambda_L$, and through the action of the Lorentz force acquire counterclockwise momentum, creating the Meissner current [162]. The orbit expansion expels negative charge, so there is a normal electron backflow to preserve charge neutrality. The forces acting on these backflowing electrons are the same as shown in the Hall bar example earlier, Fig. 9(c), and momentum is transferred to the body through the “Ampere force”, as in Fig. 9. The normal electrons have to have negative effective mass. The right panel shows the same process showing the flow of normal charge as outgoing holes, with electric and magnetic forces balanced as in Fig. 9(b).

How the electrons becoming superconducting acquire the momentum of the Meissner current is shown in Fig. 25 [162]. A microscopic orbit expanding to radius $2\lambda_L$ in the presence of magnetic field H acquires azimuthal velocity

$$v_s = -\frac{e\lambda_L}{m_e c} H \quad (42)$$

which is the speed of the electrons in the Meissner current.

So how does the system overcome Faraday’s law? Faraday’s law opposes changes in magnetic flux in the interior of a conducting material, the more so the more conducting the material is. In fig. 24, the Faraday electric field points in direction such that it pushes the supercurrent to stop and the positive ions in the body to rotate in counterclockwise direction, opposite to what they do. Yet both the electrons and the ions do exactly the opposite. The key to explain this is the radial flow. If there is no radial flow of charge, the magnetic field cannot be expelled.

An equivalent way to understand the physics of the Meissner effect is through Alfvén’s theorem of magnetohydrodynamics. It expresses the fact that in a perfectly conducting fluid, magnetic field lines are ‘frozen’ in the fluid and move together with the fluid [166], as a consequence of Faraday’s law, and magnetic field lines move without causing dissipation of Joule heat. It naturally follows that in the reversible normal-superconductor transition in a magnetic field, the magnetic field lines move out because there is outward motion of a fluid, as shown schematically in Fig. 26. In order for magnetic field lines to move out without causing a large mass or charge deficit in the interior, the fluid that moves out has to be both charge and mass neutral. That is precisely what happens in the scenario discussed here, the outward motion of negative electrons and positive holes carries no net charge nor mass.

Conventional BCS theory does not describe radial flow of anything when a system goes from the normal to the superconducting state in the presence of a magnetic field. Nor does it require hole carriers, to transfer momentum between electrons and the body in a reversible way as required by thermodynamics and experiment. Therefore,

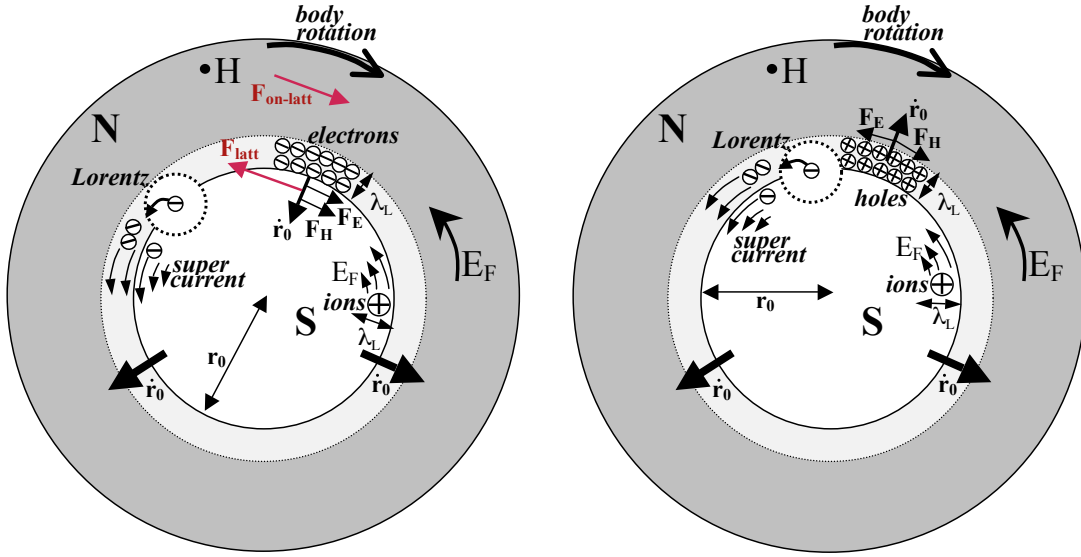


FIG. 24: Normal to superconductor transition in a magnetic field. The Faraday electric field points counterclockwise, opposing the expulsion of magnetic field. The body acquires clockwise momentum through the forces acting on the backflowing normal electrons. The left panel shows the normal backflow of electrons, the right panel shows the same with outflowing holes. Forces are balanced as in Figs. 9 (b) and 8 (c).

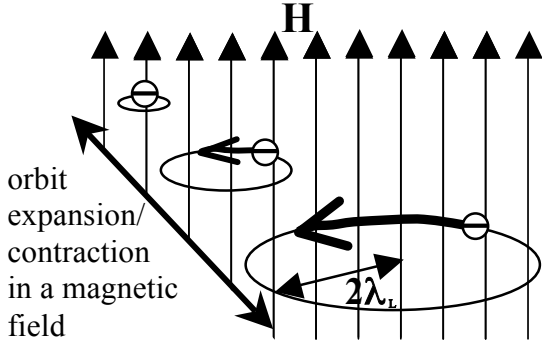


FIG. 25: Electrons expanding their orbits to radius $2\lambda_L$ in a magnetic field H perpendicular to the orbit acquire azimuthal speed Eq. (42) through the action of the Lorentz force.

conventional BCS superconductors cannot expel magnetic fields when they go superconducting, they don't have the physics required to do that. Therefore, they cannot be superconductors. Therefore, hydrides under pressure are not superconductors.

Rotating superconductors (ref. [154], p. 78) are explained by the same physics, in what is perhaps an even more transparent form [167]. Consider a rotating hollow cylinder as shown on the left panel of Fig. 27. Upon cooling into the superconducting state, it is observed that a magnetic field develops in the annulus, which results from electrons near the outer surface slowing down and electrons near the inner surface speeding up. The dynamics of this process is simply explained through the expansion of the electronic orbits to radius $2\lambda_L$ shown in Fig.

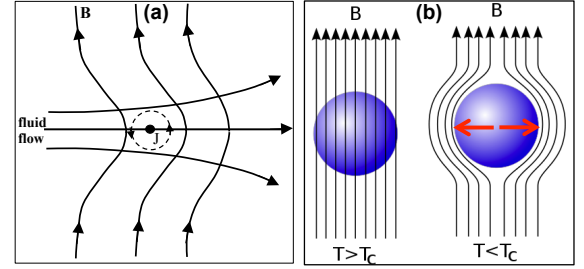


FIG. 26: The left panel shows an example illustrating Alfvén's theorem for a conducting fluid [166]. Fluid flow across magnetic field lines causes the field lines to bow out. The right panel shows the Meissner effect in a superconductor. The red arrows show the hypothesized motion of fluid, by analogy to the left panel.

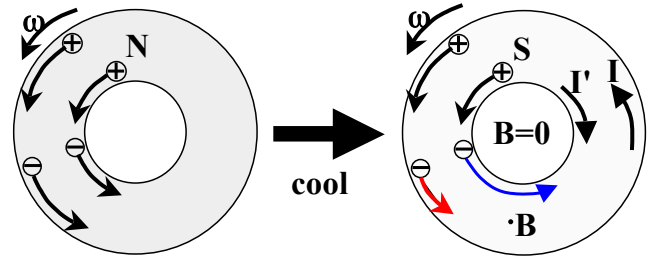


FIG. 27: Left panel: rotating hollow normal metal in the absence of applied fields. Electrons and ions move at the same speed. When the system is cooled into the superconducting state while rotating, a magnetic field develops in the interior resulting from electrons near the outer (inner) surface slowing down (speeding up).

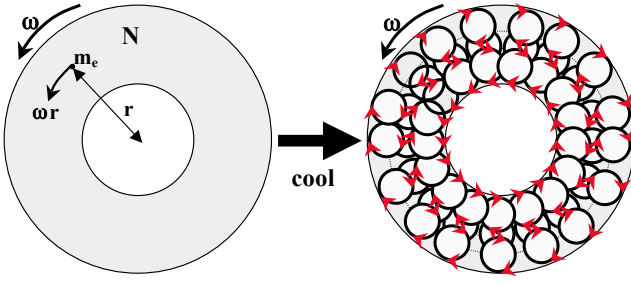


FIG. 28: Explanation of the process by which electrons near the outer and inner surface change their speeds as the rotating hollow cylinder is cooled into the superconducting state, by expansion of the orbits to radius $2\lambda_L$ as depicted in Fig. 26.

25. As shown schematically in Fig. 28, expansion of the orbits together with conservation of angular momentum causes electrons to slow down near the outer surface and speed up near the inner surface, as observed. The magnitude of the observed magnetic field is exactly given by this process, as discussed in ref. [167]. The conventional theory of superconductivity does not provide a dynamical explanation of these processes.

XII. BCS THEORY AND THE MEISSNER EFFECT

It is generally believed that BCS theory explains the Meissner effect. Instead, I have argued in the previous sections that BCS theory does not have the necessary physical elements to account for the Meissner effect. A material described by BCS theory would keep magnetic fields out if they are applied after the system is in the BCS state, however it will not expel a magnetic field from its interior in the transition from the normal to the BCS state.

Why does the physics community believe otherwise? Let us review how the Meissner effect is explained within BCS theory [1]. One considers the linear response of a system *that is already in the BCS state* to the perturbation created by a magnetic field, as shown in Fig. 29. The perturbing Hamiltonian is the linear term in the magnetic vector potential \vec{A} that results from the kinetic energy $(\vec{p} - (e/c)\vec{A})^2/2m$, and has the form

$$H_1 = \frac{ie\hbar}{2mc} \sum_i (\vec{\nabla}_i \cdot \vec{A} + \vec{A} \cdot \vec{\nabla}) \quad (43)$$

This perturbation causes the BCS wavefunction $|\Psi_G\rangle$ to become, to first order in \vec{A}

$$|\Psi\rangle = |\Psi_G\rangle - \sum_n \frac{\langle \Psi_n | H_1 | \Psi_G \rangle}{E_n} |\Psi_n\rangle \quad (44)$$

where $|\Psi_n\rangle$ are states obtained from the BCS state $|\Psi_G\rangle$ by exciting 2 quasiparticles, and E_n is the excitation energy. The expectation value of the electric current

operator with this wave function gives the electric current \vec{J} :

$$\vec{J} = \langle \Psi | \vec{J}_{op} | \Psi \rangle = -\frac{c}{4\pi} K \vec{A} \quad (45a)$$

where K is the London Kernel. I have omitted wavevector dependence here for simplicity. In the long wavelength limit this calculation yields [1]

$$K = \frac{1}{\lambda_L^2} \quad (45b)$$

where λ_L is the London penetration depth. Eq. (45) is the (second) London equation. In combination with Ampere's law, Eq. (45) predicts that the magnetic field does not penetrate the superconductor beyond a distance λ_L from the surface, where the current \vec{J} circulates, as shown schematically in Fig. 29 right panel.

This calculation uses only the BCS wavefunction in and around the BCS state, namely the ground state wavefunction $|\Psi_G\rangle$ and the wavefunctions $|\Psi_n\rangle$ that result from breaking one Cooper pair at a time. The wavefunction of the normal metal never appears in this calculation.

That is *not* explaining the Meissner effect. The Meissner effect is what is shown in Fig. 30: the process by which a system starting in the normal metallic state expels a magnetic field in the process of becoming a superconductor. It cannot be explained by starting from the assumption that the system is in the final BCS state and gets perturbed by H_1 . Explaining this process requires explaining how the interface between normal and superconducting regions moves (center panel in Fig. 30), satisfying conservation laws, thermodynamic constraints, and Faraday's law. That is what we explained within the theory of hole superconductivity in the previous sections. It required radial flow of charge, which BCS theory does not predict.

Maybe the reader will think: when the system is cooled, the normal state wavefunction somehow turns into the BCS wavefunction, and then the perturbing Hamiltonian H_1 acts and the magnetic field gets expelled according to the calculation above. However that cannot be so: the BCS state $|\Psi_G\rangle$ has global phase coherence, and phase coherence cannot exist in the presence of a magnetic field in the interior of the system. So the system cannot go into the BCS state in the presence of the magnetic field. It has to evolve into the superconducting state as it expels the magnetic field. Calculations of the sort described in Eqs. (41)-(43) contain no information about what is the nature of the initial state when the Meissner effect starts, the normal metal, so they cannot be a microscopic derivation of the Meissner effect.

If BCS does not have the physical elements that are necessary to describe the Meissner effect, it cannot be the correct theory for the equilibrium state of superconductors either, even if it does describe *some* of their properties, e.g. the existence of an energy gap. Therefore it cannot be used to describe real superconductors, nor to predict which materials will be superconducting.

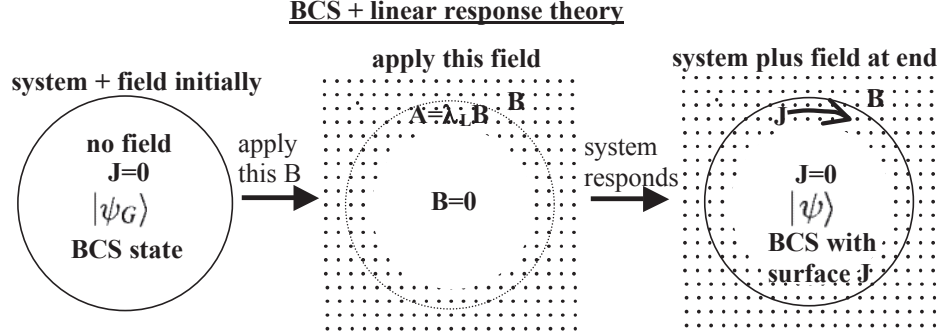


FIG. 29: The BCS view of the Meissner effect. In the BCS explanation of the Meissner effect, the system (cylinder, top view) is in the BCS state (left panel) initially with no magnetic field, and its linear response to the magnetic field shown in the middle panel (dots) is computed to first order in the magnetic field. The result is the state shown in the right panel, with a surface current J circulating.

XIII. SUPERCONDUCTING MATERIALS

The theory discussed in this Tutorial leads to the following clear criteria:

1. If a material does not have hole carriers in the normal state it cannot become superconducting at any temperature.
2. Highest T_c 's result when holes conduct through negatively charged anions

There is a lot of evidence from superconducting ma-

terials that these criteria are correct. We already discussed some of that evidence in Sect. III. Reference [168] lists and discusses many examples. A particularly clear example is MgB_2 , universally believed to be a "conventional superconductor". Figure 31 shows the bandstructure, from calculations by Kortus et al [169]. There are hole carriers at the Γ point, indicated by the red arrow, that correspond to holes conducting in the planar array of B^- anions through direct hopping between them, precisely what the theory says is needed for high temperature superconductivity. The same physics explains the

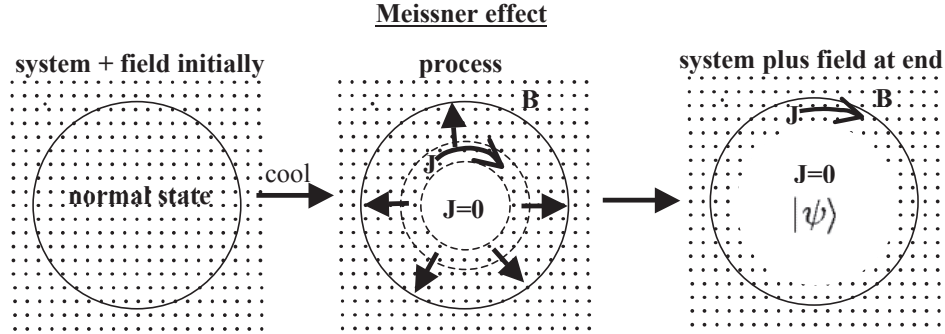


FIG. 30: What the Meissner effect really is: the *process* by which a normal metal becomes superconducting in the presence of a magnetic field throughout its interior initially. The simplest route in this process (not the only one) is depicted in the figure. The superconducting region (white region) expands gradually from the center to fill the entire volume, expelling the magnetic field in the process.

high T_c of the cuprates, with holes hopping through the O^\ominus anions in the copper-oxygen planes [139, 146, 171].

Another clear example is superconductivity in $FeSe$. It is observed that the critical temperature increases sharply from 8K to 37K under application of pressure. From the measured interatomic distances we conclude as shown in Fig. 32 that the overlap between the Se^\ominus anions increases, giving rise to a substantial increase in Δt (that depends exponentially on the distance between anions) and consequently a much higher T_c .

How do hydrides under pressure satisfy the criteria 1.

and 2. given above? They clearly don't. A hydrogen-rich material cannot have hole carriers conducting through negatively charged anions, as the cuprates, pnictides, and MgB_2 do. The metal atom in e.g. LaH_{10} does not have enough electrons to convert all the surrounding H atoms into H^- ions. Nor can it work by hydrogen atoms donating electrons to the metal atoms making them into negative anions, and holes conducting through direct hopping between the anions: they are too far apart and there are hydrogen ions in the way.

For a while we thought that an exception could be

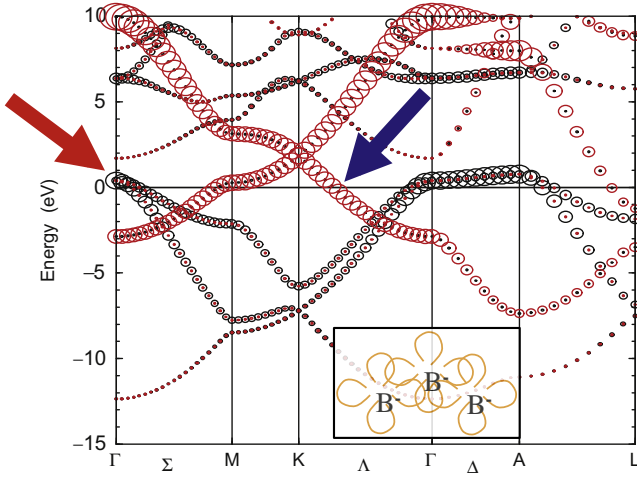


FIG. 31: Band structure of MgB_2 from ref. [169] reproduced with the permission of AIP Publishing. Conduction occurs through holes in the pocket near the C point indicated by the red arrow. The blue arrow shows a three-dimensional band where the carriers are electron-like. The inset shows schematically the boron p_{xy} orbitals in the B planes, where conduction occurs through holes in the pocket near the C point indicated by the red arrow on the right panel.

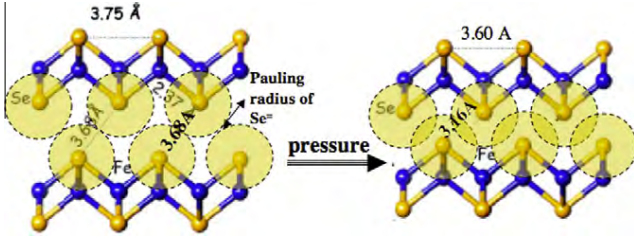


FIG. 32: Schematic depiction of FeSe planes without (left) and with (right) application of pressure (part of this figure was reproduced from Ref. [170], Fig. 4(d) with the permission of AIP Publishing). The main effect of pressure is to reduce the $Se^{=}-Se^{=}$ distance between $Se^{=}$ anions in neighboring planes, leading to substantial overlap of anion orbitals.

H_2S . Right after the initial results were announced [172] we wrote a paper [173] proposing that the initial observations by Eremets et al could be explained by holes conducting through negatively charged $S^{=}$ anions in H_2S . When it became clear that the structure giving rise in appearance to high T_c superconductivity was H_3S rather than H_2S it became clear to us that the claimed superconductivity of sulfur hydride does not satisfy the criteria discussed here and therefore it could not be superconductivity.

XIV. CONCLUSION

The battle of Austerlitz was Napoleon's greatest triumph in his quest to conquer Europe, then in Waterloo he met his final defeat. I predict that hydride supercon-

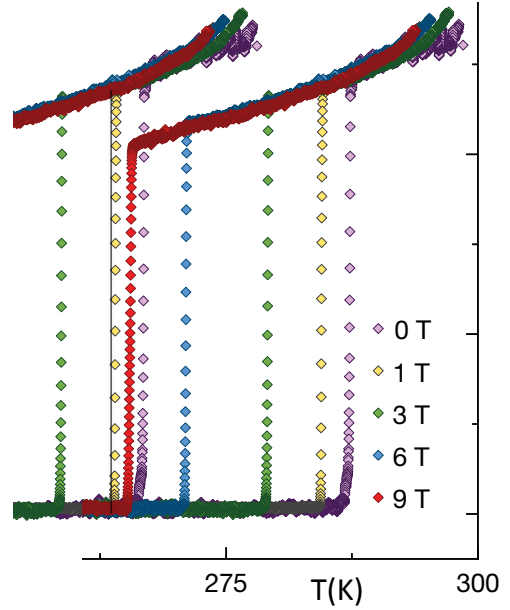


FIG. 33: Resistance versus temperature in the presence of a magnetic field for CSH, from ref. [29] reproduced with permission from Nature Publishing, copyright 2021 Nature Publishing. The image was copied and shifted horizontally to illustrate the absence of any broadening of the transition for magnetic field 9 T (red points) versus the transitions for 0 T and 1 T (purple and yellow points). The thin black line next to the yellow points is vertical.

ductivity will be both Austerlitz and Waterloo for BCS-electron-phonon theory. As of the writing of this Tutorial we are in the aftermath of Austerlitz, at the end of the beginning [93, 174] on the way to Waterloo.

In closing I would like to focus again on the extreme narrowness of the resistive transitions [93] for the alleged room temperature superconductor carbonaceous sulfur hydride (CSH) reported in ref. [29] that we discussed in Sect. II of this Tutorial. The resistance curves are shown in Fig. 33. It is contrary to everything we know about superconductivity [1], whether conventional or unconventional, that a superconducting transition at this high temperature for a strongly type II material would show absolutely no broadening in a magnetic field as large as 9 T. The anomaly is compounded by the fact that this is supposed to be a conventional superconductor, about which we should know so much [1]. Barring the highly unlikely possibility that CSH is a “nonstandard superconductor” [94], qualitatively different from both conventional and unconventional superconductors, this indicates that CSH *is not* a superconductor. The superconductivity of CSH has also recently been called into question for theoretical reasons based on the conventional theory [83, 175].

And, if CSH is not a superconductor, it teaches us something very important. That a hydrogen-rich material under high pressures will display drops in resistance that shift downward in temperature when a mag-

netic field is applied, for reasons unrelated to superconductivity. Whatever physics or experimental artifact is responsible for this behavior, if it happens for CSH it can happen also for the other 11 hydrogen-rich materials under high pressure that have been claimed to be high temperature superconductors [18–34] and account for the observations there. As recounted in Sect. II, much of the experimental evidence for superconductivity in these materials has recently been called into question.

The scientific community has adopted as an article of faith that there is more than one mechanism of superconductivity in nature. That has to be true if BCS theory describes some superconducting materials, but not if it describes none. Before 1957 it was certainly generally expected that a single theory would describe all superconductivity in nature, and for many years after 1957 it was believed that that single theory was BCS. It was only when superconducting materials that couldn’t possibly be described by BCS theory were discovered in the late 70’s and mid 80’s that the scientific world embraced polytheism, without even knowing who the other gods are. The alternative to stick to monotheism and discard a false BCS god [36] was never considered. I argue that that alternative has become increasingly compelling, given the proliferation of classes of materials classified as “unconventional superconductors” in recent years [84]. The consensus today, that if a newly discovered superconductor does not fit the BCS framework it is classified as “unconventional”, rather than casting doubt on the validity of BCS, is highly anomalous. BCS has become a theory that cannot be falsified, which by definition makes it unscientific [176].

Furthermore, a hallmark of valid scientific theories is their ability to predict. If the predicted phenomena are subsequently observed, they lend credibility to the theory, particularly if the predicted phenomena were unexpected. As the other side of the same coin, if the predicted phenomena are not observed this undermines the claim to validity of the theory. Strangely, for the case of BCS theory there have been myriads of predictions of superconducting materials that have *not* been verified, yet for some reason this has not undermined the faith of the scientific community in the validity of BCS theory.

Hydride superconductors provide a unique opportunity, because they have been hailed as a poster child for the physics proposed by BCS to give rise to high temperature superconductivity, namely light ionic mass and strong electron-phonon coupling. Instead, the theory of hole superconductivity reviewed here predicts that high temperature superconductivity in pressurized hydrides does not exist. In the not too distant future, experimentalists looking at their experimental results with an open mind unclouded by the prejudice that BCS theory has to be correct, will hopefully determine unequivocally and reproducibly what is the true state of affairs.

So, if hydride high temperature superconductivity in-

deed is real, the theory of hole superconductivity will be proven wrong, and this will confirm that the universal belief in the validity of BCS theory is indeed correct, and, unfortunately for Occam’s razor, that more than one mechanism is needed to describe superconductivity in nature.

But, if hydride high temperature superconductivity is found not to exist, BCS theory should be discarded as a descriptor of the superconductivity of real materials. If it can’t predict superconductivity even in the hydrides, it will be clear evidence that the electron-phonon interaction is not the cause of superconductivity in any of the other 11 classes of superconducting materials currently considered to be “conventional superconductors” [84] either. This will allow the possibility that those 11 classes, as well as the other 21 classes of materials currently believed to be either certainly or possibly non-BCS superconductors [84], may be described by a single mechanism of superconductivity. Occam’s razor will prevail.

And, since the theory of hole superconductivity predicts that no high temperature superconductivity exists in pressurized hydrides, if this is proven to be correct it will be confirmation of an unexpected prediction and therefore add support to the possibility that its fundamental principles [177] reviewed in this Tutorial are an essential part of a valid description of the superconductivity of all materials.

Acknowledgments

I am grateful to Frank Marsiglio for collaboration in several parts of the work reviewed here. I would also like to acknowledge helpful discussions and information received on various aspects of hydride superconductivity with/from D. Semenov, S. Shylin, M. Erements, S. Budko, V. Minkov, T. Timusk, R. Pascale, X. Huang, T. Cui, J. J. Hamlin, V. Struzhkin, J. Cheng, R. Hemley, M. Nuñez-Regueiro, J. Flores Livas, E. Zurek, M. L. Cohen, I. Felner, E. Talantsev, I. Bozovic, H. R. Ott, T. Forgan, M. Debessai, J. Schilling, K. Shimizu, S. K. Sinha, M. B. Maple and N. W. Ashcroft.

Note added: While this paper was being reviewed, a new paper by Erements and coworkers reporting magnetic measurements on H_3S and LaH_{10} was posted on-line [178], claiming that they show “definitive evidence for the Meissner effect”. Instead, we argue that it provides clear evidence *against* the existence of high temperature superconductivity in pressurized hydrides [179].

Data availability statement: The data that support the findings of this study are available from the author upon reasonable request.

-
- [1] M. Tinkham, "Introduction to superconductivity", Second Edition, McGraw Hill, New York, 1996.
 - [2] C. J. Pickard, I. Errea and M. I. Erements, "Superconducting Hydrides Under Pressure", *Ann. Rev. Cond. Matt. Phys.* **11**, 57 (2020) and references therein.
 - [3] R. F. Service, "Feeling the pressure", *Science* **373**, 954 (2021).
 - [4] J. Lv, Y. Sun, H. Liu and Y. Ma, "Theory-orientated discovery of high-temperature superconductors in superhydrides stabilized under high pressure", *Matter and Radiation at Extremes* **5**, 068101 (2020) and references therein.
 - [5] J. A. Flores-Livas et al., "A perspective on conventional high-temperature superconductors at high pressure: Methods and materials", *Physics Reports* **856**, 1 (2020).
 - [6] L. Boeri et al, "The 2021 Room-Temperature Superconductivity Roadmap", *J. Phys. Cond. Matt.*, to be published.
 - [7] See <https://jorge.physics.ucsd.edu/hole.html> for a list of references.
 - [8] J. E. Hirsch, "Hole superconductivity", *Phys. Lett. A* **134**, 451 (1989).
 - [9] B. T. Matthias, "Anticorrelations in superconductivity", *Physica* **55**, 69 (1972).
 - [10] M. L. Cohen, "Predicting and explaining T_c and other properties of BCS superconductors", *Mod. Phys. Lett. B* **24**, 2755 (2010). See first paragraph of Sect. 3.
 - [11] Y. Li et al, "The metallization and superconductivity of dense hydrogen sulfide", *J. Chem. Phys.* **140**, 174712 (2014).
 - [12] A.P. Drozdov, M.I. Erements, I. A. Troyan, V. Ksenofontov and S. I. Shylin, "Conventional superconductivity at 203 kelvin at high pressures in the sulfur hydride system", *Nature* **525**, 73-76 (2015).
 - [13] N. W. Ashcroft, "Metallic Hydrogen: A High-Temperature Superconductor?", *Phys. Rev. Lett.* **21**, 1748 (1968).
 - [14] N. W. Ashcroft, "Hydrogen Dominant Metallic Alloys: High Temperature Superconductors?", *Phys. Rev. Lett.* **92**, 187002 (2004).
 - [15] V. V. Struzhkin, "Superconductivity in compressed hydrogen-rich materials: Pressing on hydrogen", *Physica C* **514**, 77 (2015).
 - [16] T. Bi, N. Zarifi, T. Terpstra and E. Zurek, "The Search for Superconductivity in High Pressure Hydrides", [arXiv:1806.00163](https://arxiv.org/abs/1806.00163) (2018), *Reference Module in Chemistry, Molecular Sciences and Chemical Engineering* (2019) and references therein.
 - [17] H. Nakao et al, "Superconductivity of Pure H_3S Synthesized from Elemental Sulfur and Hydrogen", *J. Phys. Soc. Jpn* **88**, 123701 (2019).
 - [18] A.P. Drozdov, M. I. Erements and I. A. Troyan, "Superconductivity above 100 K in PH₃ at high pressures", [arXiv:1508.06224](https://arxiv.org/abs/1508.06224) (2015).
 - [19] A.P. Drozdov et al., "Superconductivity at 250 K in lanthanum hydride under high pressures", *Nature* **569**, 528 (2019).
 - [20] F. Hong et al, "Superconductivity of Lanthanum Superhydride Investigated Using the Standard Four-Probe Configuration under High Pressures", *Chin. Phys. Lett.* **37**, 107401 (2020).
 - [21] M. Somayazulu et al., "Evidence for superconductivity above 260 K in lanthanum superhydride at megabar pressures", *Phys. Rev. Lett.* **122**, 027001 (2019).
 - [22] A. D. Grockowiak et al, "Hot Hydride Superconductivity above 550 K", [arXiv:2006.03004](https://arxiv.org/abs/2006.03004) (2020).
 - [23] P. P. Kong et al, "Superconductivity up to 243 K in yttrium hydrides under high pressure", [arXiv:1909.10482](https://arxiv.org/abs/1909.10482) (2019).
 - [24] Y. A. Troyan et al., "Anomalous high-temperature superconductivity in YH_6 ", *Adv. Mater.* **33**, 2006832 (2021).
 - [25] E. Snider et al, "Synthesis of Yttrium Superhydride Superconductor with a Transition Temperature up to 262 K by Catalytic Hydrogenation at High Pressures", *Phys. Rev. Lett.* **126**, 117003 (2021).
 - [26] D. V. Semenov et al., "Superconductivity at 161 K in thorium hydride ThH_{10} : Synthesis and properties", *Materials Today* **33**, 36 (2020).
 - [27] D. Zhou et al, "Superconducting praseodymium superhydrides", *Science Advances* **6**, eaax6849 (2020).
 - [28] D. V. Semenov et al, "Superconductivity at 253 K in lanthanum-yttrium ternary hydrides", [arXiv:2012.04787](https://arxiv.org/abs/2012.04787) (2020).
 - [29] E. Snider et al., "Room-temperature superconductivity in a carbonaceous sulfur hydride", *Nature* **586**, 373 (2020).
 - [30] W. Chen et al, "High-Temperature Superconductivity in Cerium Superhydrides", [arXiv:2101.01315](https://arxiv.org/abs/2101.01315) (2021).
 - [31] F. Hong et al, "Superconductivity at 70 K in Tin Hydride SnH_x under High Pressure", [arXiv:2101.02846](https://arxiv.org/abs/2101.02846) (2021).
 - [32] W. Chen et al, "Synthesis of molecular metallic barium superhydride: pseudocubic BaH_{12} ", *Nature Comm.* **12**, 273 (2021).
 - [33] L. Ma et al, "Experimental observation of superconductivity at 215K in calcium superhydride at high pressures", [arXiv:2103.16282](https://arxiv.org/abs/2103.16282) (2021).
 - [34] Z. W. Li et al, "Superconductivity above 200K Observed in Superhydrides of Calcium", [arXiv:2103.16917](https://arxiv.org/abs/2103.16917) (2021).
 - [35] G. Gao et al, "Superconducting Binary Hydrides: Theoretical Predictions and Experimental Progresses", *Materials Today Physics* **100546** (2021).
 - [36] J. E. Hirsch, "BCS theory of superconductivity: it is time to question its validity", *Phys. Scripta* **80**, 035702 (2009).
 - [37] H. Wang et al, "Superconductive sodalite-like clathrate calcium hydride at high pressures", *PNAS* **109**, 6463 (2012).
 - [38] J. Hooper et al, "Polyhydrides of the Alkaline Earth Metals: A Look at the Extremes under Pressure", *J. Phys. Chem. C* **117**, 2982 (2013).
 - [39] D. Duan et al, "Pressure-induced metallization of dense $(H_2S)_2H_2$ with high- T_c superconductivity", *Sci. Rep.* **4**, 6968 (2015).
 - [40] Y. Fu et al, "High-Pressure Phase Stability and Superconductivity of Pnictogen Hydrides and Chemical Trends for Compressed Hydrides", *Chem. Mater.* **28**, 1746 (2016).
 - [41] D. Duan et al, "Structure and superconductivity of hydrides at high pressures", *National Science Review* **4**,

- 121 (2017).
- [42] F. Peng et al, “Hydrogen Clathrate Structures in Rare Earth Hydrides at High Pressures: Possible Route to Room-Temperature Superconductivity”, *Phys. Rev. Lett.* **119**, 107001 (2017).
 - [43] A. Shamp and E. Zurek, “Superconductivity in Hydrides Doped with Main Group Elements Under Pressure”, *Novel Superconducting Materials*, **3**, 14 (2017).
 - [44] H. Liu et al, “Potential high- T_c superconducting lanthanum and yttrium hydrides at high pressure”, *PNAS* **114** 6990 (2017).
 - [45] I. A. Kruglov et al, “Uranium polyhydrides at moderate pressures: Prediction, synthesis, and expected superconductivity”, *Science Advances* **4**, eaat9776 (2018).
 - [46] L. P. Gor’kov and V. Z. Kresin, “High pressure and road to room temperature superconductivity”, *Rev. Mod. Phys.* **90**, 011001 (2018).
 - [47] L. Boeri and B. Bachelet, “Viewpoint: the road to room-temperature conventional superconductivity”, *J. Phys. Cond. Matt.* **31**, 234002 (2019).
 - [48] Y. Quan, S. S. Ghosh, and W. E. Pickett, “Compressed hydrides as metallic hydrogen superconductors”, *Phys. Rev. B* **100**, 184505 (2019).
 - [49] E. Zurek and T. Bi, “High-temperature superconductivity in alkaline and rare earth polyhydrides at high pressure: A theoretical perspective”, *J. Chem. Phys.* **150**, 050901 (2019).
 - [50] Y. Sun et al, “Route to a Superconducting Phase above Room Temperature in Electron-Doped Hydride Compounds under High Pressure”, *Phys. Rev. Lett.* **123**, 097001 (2019).
 - [51] V. Struzhkin et al, “Superconductivity in La and Y hydrides: Remaining questions to experiment and theory”, *Matter and Radiation at Extremes* **5**, 028201 (2020), Fig. 8.
 - [52] D. V. Semenov et al, “On Distribution of Superconductivity in Metal Hydrides”, *Current Opinion in Solid State and Materials Science* **24**, 100808 (2020) and references therein.
 - [53] J. Lv, Y. Sun, H. Liu and Y. Ma, “Theory-orientated discovery of high-temperature superconductors in superhydrides stabilized under high pressure”, *Matter and Radiation at Extremes* **5**, 068101 (2020).
 - [54] M. Du et al, “High-temperature superconductivity in transition metallic hydrides MH_{11} ($M = \text{Mo, W, Nb, and Ta}$) under high pressure”, *Phys. Chem. Chem. Phys.*, **23**, 6717 (2021).
 - [55] A. M. Shipley, M. J. Hutcheon, R. J. Needs and C. J. Pickard, “High-throughput discovery of high-temperature conventional superconductors”, [arXiv:2105.02296](https://arxiv.org/abs/2105.02296) (2021).
 - [56] J. N. Wang et al, “High-temperature superconductivity in SrB_3C_3 and BaB_3C_3 predicted from first-principles anisotropic Migdal-Eliashberg theory”, *Phys. Rev. B* **103**, 144515 (2021).
 - [57] V. Sadovskii, “Limits of Eliashberg Theory and Bounds for Superconducting Transition Temperature”, [arXiv:2106.0994](https://arxiv.org/abs/2106.0994).
 - [58] Ref. [12], that launched the field in 2015, has to date (August 2021) 1573 citations in Google Scholar, essentially all of which assume that superconductivity in these materials is real and base the research reported in those papers on that assumption.
 - [59] T. Durakiewicz, T. Oder, D. Hess, D. Rabson, B. Schwenzer, R. Meulenberg and S. L. Jones, National Science Foundation “Dear Colleague Letter: Funding Opportunity - Light and Warm Superconductors”, *NSF* **21-039**, January 27, 2021.
 - [60] M. I. Eremets et al, “Superconductivity in Hydrogen Dominant Materials: Silane”, *Science* **319**, 1506 (2008).
 - [61] J. Feng et al, “Structures and Potential Superconductivity in SiH_4 at High Pressure: En Route to “Metallic Hydrogen””, *Phys. Rev. Lett.* **96**, 017006 (2006).
 - [62] C. J. Pickard and R. J. Needs, “High-Pressure Phases of Silane”, *Phys. Rev. Lett.* **97**, 045504 (2006).
 - [63] Y. Yao et al, “Superconductivity in high-pressure SiH_4 ”, *Europhys. Lett.* **78**, 37003 (2007).
 - [64] X. Jin et al, “Superconducting high-pressure phases of disilane”, *PNAS* **22**, 9969 (2010).
 - [65] J. S. Tse, Y. Yao and K. Tanaka, “Novel Superconductivity in Metallic SnH_4 under High Pressure”, *Phys. Rev. Lett.* **98**, 117004 (2007).
 - [66] I. Goncharenko et al, “Pressure-Induced Hydrogen-Dominant Metallic State in Aluminum Hydride”, *Phys. Rev. Lett.* **100**, 045504 (2008).
 - [67] Y. Xie, Q. Li, A. R. Oganov and H. Wang, “Superconductivity of lithium-doped hydrogen under high pressure”, *Acta Crystallogr C Struct Chem* **70**, 104 (2014).
 - [68] D. Zhou et al, “Ab initio study revealing a layered structure in hydrogen-rich KH_6 under high pressure”, *Phys. Rev. B* **86**, 014118 (2012).
 - [69] Z. Wang et al, “Metallization and superconductivity of BeH_2 under high pressure”, *J. Chem. Phys.* **140**, 124707 (2014).
 - [70] X. Feng et al, “Compressed sodalite-like MgH_6 as a potential high temperature superconductor”, *RSC Adv.* **5**, 59292 (2015).
 - [71] S. Zhang et al, “Phase Diagram and High-Temperature Superconductivity of Compressed Selenium Hydrides”, *Scientific Reports* **5**, 15433 (2015).
 - [72] J. A. Flores-Livas, A. Sanna and E.K.U. Gross, “High temperature superconductivity in sulfur and selenium hydrides at high pressure”, *Eur. Phys. J. B* **89**, 63 (2016).
 - [73] X. Zhong et al, “Tellurium Hydrides at High Pressures: High-Temperature Superconductors”, *Phys. Rev. Lett.* **116**, 057002 (2016).
 - [74] X. Li and F. Peng, “Superconductivity of Pressure-Stabilized Vanadium Hydrides”, *Inorg. Chem.* **56**, 13759 (2017).
 - [75] G. Gao et al, “Theoretical study of the ground-state structures and properties of niobium hydrides under pressure”, *Phys. Rev. B* **88**, 184104 (2013).
 - [76] Y. Fu et al, “High-Pressure Phase Stability and Superconductivity of Pnictogen Hydrides and Chemical Trends for Compressed Hydrides”, *Chem. Mater.* **28**, 1746 (2016).
 - [77] X. Ye et al, “High Hydrides of Scandium under Pressure: Potential Superconductors”, *J. Phys. Chem. C* **122**, 6298 (2018).
 - [78] I. A. Kruglov et al, “Uranium polyhydrides at moderate pressures: Prediction, synthesis, and expected superconductivity”, *Science Advances* **4**, eaat9776 (2018).
 - [79] S. Yu et al, “Pressure-driven formation and stabilization of superconductive chromium hydrides”, *Scientific Reports* **5**, 17764 (2015).
 - [80] S. Zheng et al, “Structural and Superconducting Properties of Tungsten Hydrides Under High Pressure”,

- Front. Phys. 6, 101 (2018).
- [81] D. V. Semenok et al, “Actinium Hydrides AcH_{10} , AcH_{12} , and AcH_{16} as High-Temperature Conventional Superconductors”, *J. Phys. Chem. Lett.* 9, 1920 (2018).
 - [82] X. Wang et al, “A Little Bit of Carbon Can do a Lot for Superconductivity in H_3S ”, [arXiv:2109.09898 \(2021\)](#).
 - [83] M. Gubler et al, “Missing theoretical evidence for conventional room temperature superconductivity in low enthalpy structures of carbonaceous sulfur hydrides”, [arXiv:2109.10019 \(2021\)](#).
 - [84] Physica C Special Issue, “Superconducting Materials: Conventional, Unconventional and Undetermined. Dedicated to Theodore H. Geballe on the year of his 95th birthday”, ed. by J.E. Hirsch, M.B. Maple, F. Marsiglio, Vol. 514, 1-444 (2015).
 - [85] J. E. Hirsch, M. B. M. Maple and F. Marsiglio, “Superconducting materials classes: Introduction and overview”, *Physica C* 514, 1 (2015).
 - [86] P. B. Allen, “Isotope shift controversies”, *Nature* 335, 396 (1988).
 - [87] R. D. Fowler, J. D. G. Lindsay, R. W. White, H. H. Hill and B. T. Matthias, “Positive isotope effect on the superconducting transition temperature of α -uranium”, *Phys. Rev. Lett.* 19, 892 (1967).
 - [88] B. Stritzker and W. Buckel, “Superconductivity in the palladium-hydrogen and the palladium-deuterium systems”, *Z. Physik* 257, 1 (1972).
 - [89] D. A. Papaconstantopoulos, B. M. Klein, E. N. Economou and L. L. Boyer, “Band structure and superconductivity of PdD_x and PdH_x ”, *Phys. Rev. B* 17, 141 (1978).
 - [90] I. Errea et al, “High-Pressure Hydrogen Sulfide from First Principles: A Strongly Anharmonic Phonon-Mediated Superconductor”, *Phys. Rev. Lett.* 114, 157004 (2015).
 - [91] E. E. Haller, “Isotopically controlled semiconductors”, *Solid State Commun.* 133, 693 (2005).
 - [92] J. E. Hirsch and F. Marsiglio, “Absence of high temperature superconductivity in hydrides under pressure”, [arXiv:2010.10307 \(2020\)](#).
 - [93] J. E. Hirsch and F. Marsiglio, “Unusual width of the superconducting transition in a hydride”, *Nature* 596, E9 (2021).
 - [94] J. E. Hirsch and F. Marsiglio, “Nonstandard superconductivity or no superconductivity in hydrides under high pressure”, *Phys. Rev. B* 103, 134505 (2021).
 - [95] M. Debessai, T. Matsuoka, J. J. Hamlin, J. S. Schilling and K. Shimizu, “Pressure-Induced Superconducting State of Europium Metal at Low Temperatures”, *Phys. Rev. Lett.* 102, 197002 (2009).
 - [96] J. E. Hirsch, “On the ac magnetic susceptibility of a room temperature superconductor: anatomy of a probable scientific fraud”, *Physica C* [doi.org/10.1016/j.physc.2021.1353964 \(2021\)](#).
 - [97] J. E. Hirsch, “About the Pressure-Induced Superconducting State of Europium Metal at Low Temperatures”, *Physica C* 583, 1353805 (2021).
 - [98] See “30 August 2021 Editor’s Note” in ref. [29].
 - [99] J. E. Hirsch, [arXiv:2012.07537 \(2021\)](#).
 - [100] Author of [95], private communication to author.
 - [101] X. Huang et al, “High-temperature superconductivity in sulfur hydride evidenced by alternating-current magnetic susceptibility”, *Nat. Sci. Rev.* 6, 713 (2019).
 - [102] J. E. Hirsch, “Faulty evidence for superconductivity in ac magnetic susceptibility of sulfur hydride under pressure”, [arXiv:2109.08517 \(2021\)](#).
 - [103] V. Struzhkin et al, “Superconductivity in La and Y hydrides: Remaining questions to experiment and theory”, *Matter and Radiation at Extremes* 5, 028201 (2020).
 - [104] I. Troyan et al, “Observation of superconductivity in hydrogen sulfide from nuclear resonant scattering”, *Science* 351, 1303 (2016).
 - [105] V. Struzhkin, “Squeezing into superconductivity”, *Science* 351, 1260 (2016).
 - [106] J. E. Hirsch and F. Marsiglio, “Meissner effect in non-standard superconductors”, *Physica C* 587, 1353896 (2021).
 - [107] J. E. Hirsch and F. Marsiglio, “Flux trapping in superconducting hydrides under high pressure”, *Physica C* 589, 1353916 (2021).
 - [108] J. E. Hirsch and F. Marsiglio, “Absence of magnetic evidence for superconductivity in hydrides under high pressure”, *Physica C* 584, 1353866 (2021).
 - [109] F. Capitani et al, “Spectroscopic evidence of a new energy scale for superconductivity in H_3S ”, *Nat Phys.* 13, 859 (2017).
 - [110] J. E. Hirsch and F. Marsiglio, “Absence of evidence of superconductivity in sulfur hydride in optical reflectance experiments”, [arXiv:2109.10878 \(2021\)](#).
 - [111] E. J. Nicol and J. P. Carbotte, “Comparison of pressurized sulfur hydride with conventional superconductors”, *Phys. Rev. B* 91, 220507(R) (2015).
 - [112] M. Debessai, J. J. Hamlin and J. S. Schilling, “Comparison of the pressure dependences of T_c in the trivalent d-electron superconductors Sc, Y, La, and Lu up to megabar pressures”, *Phys. Rev. B* 78, 064519 (2008).
 - [113] J.E. Hirsch and J.J. Hamlin, “Why non-superconducting metallic elements become superconducting under high pressure”, *Physica C* 470, S937 (2010).
 - [114] F. Marsiglio and J. Carbotte, in “Superconductivity”, edited by K. Bennemann and J. Ketterson, Vol. 1, p. 73 (Springer, Berlin, 2008).
 - [115] J. Bauer, J. E. Han, and O. Gunnarsson, “Retardation effects and the Coulomb pseudopotential in the theory of superconductivity”, *Phys. Rev. B* 87, 054507 (2013).
 - [116] G. W. Webb, F. Marsiglio and J. E. Hirsch, “Superconductivity in the elements, alloys and simple compounds”, *Physica C* 514, 17 (2015).
 - [117] P. B. Allen and M. L. Cohen, “Pseudopotential calculation of the mass enhancement and superconducting transition temperature of simple metals”, *Phys. Rev.* 187, 525 (1969).
 - [118] A. Y. Liu and M. L. Cohen, “Electron-phonon coupling in bcc and 9R lithium”, *Phys. Rev. B* 44, 9678 (1991).
 - [119] H. Capelmann, “Incipient antiferromagnetism in scandium”, *J. Low Temp. Phys.* 3 189 (1970).
 - [120] G. Gladstone, M. A. Jensen and J. R. Schrieffer, “Superconductivity in the Transition Metals: theory and experiment”, in “Superconductivity”, ed. by R. D. Parks, Marcel Dekker, Inc., New York, 1969, Vol. II, p. 665.
 - [121] D. Rainer, “First principles calculations of T_c in superconductors”, *Physica B* 109 & 110, 1671 (1982).
 - [122] J.E. Hirsch, “Correlations between normal-state properties and superconductivity”, *Phys. Rev. B* 55, 9007 (1997).
 - [123] J.E. Hirsch, “Hole superconductivity in MgB_2 : a high T_c cuprate without Cu”, *Phys. Lett. A* 282, 392 (2001).

- [124] J. Nagamatsu et al, “Superconductivity at 39 K in magnesium diboride”, *Nature* **410**, 63 (2001).
- [125] W. N. Kang et al, “Hole carrier in MgB_2 characterized by Hall measurements”, *App. Phys. Lett.* **79**, 982 (2001).
- [126] A. A. Manuel et al, “Contribution to the determination of the Fermi surface of V_3Si by positron annihilation”, *Sol. St. Comm.* **31**, 955 (1979); S. Berko and M. Weger, “Investigation of the Fermi Surface of V_3Si by Means of Positron Annihilation”, *Phys. Rev. Lett.* **24**, 55 (1970); L. Hoffmann, A.K. Singh, H. Takei and N. Toyota, “Fermi surfaces in Nb_3Sn through positron annihilation”, *J. Phys. F* **18**, 2605 (1988).
- [127] E. Bustarret, “Superconductivity in doped semiconductors”, *Physica C* **514**, 36 (2015).
- [128] S. Uchida et al, “Electric and Magnetic Properties of La_2CuO_4 ”, *JJAP* **26**, L445 (1987).
- [129] Y. Tokura, H. Takagi, and S. Uchida, “A superconducting copper oxide compound with electrons as the charge carriers”, *Nature* **377**, 345 (1989).
- [130] Y. Dagan and R.L. Greene, “Hole superconductivity in the electron-doped superconductor $Pr_{2-x}Ce_xCuO_4$ ”, *Phys. Rev. B* **76**, 024506 (2007).
- [131] Yangmu Li, W. Tabis, Y. Tang, G. Yu, J. Jaroszynski, N. Barisic and M. Greven, “Hole-pocket-driven superconductivity and its universal features in the electron-doped cuprates”, *Science Advances* **5**, eaap7349 (2019).
- [132] J.E. Hirsch and F. Marsiglio, “On the dependence of superconducting T_c on carrier concentration”, *Phys. Lett. A* **140**, 122 (1989); “Understanding electron-doped cuprate superconductors as hole superconductors”, *Physica C* **564**, 29 (2019).
- [133] J.E. Hirsch and F. Marsiglio, “Electron-phonon or hole superconductivity in MgB_2 ?”, *Phys. Rev. B* **64**, 144523 (2001).
- [134] J. E. Hirsch, “Momentum of superconducting electrons and the explanation of the Meissner effect”, *Phys. Rev. B* **95**, 014503 (2017).
- [135] W. H. Keesom and J. A. Kok, “Further calorimetric experiments on thallium”, *Physica* **1**, 595 (1934).
- [136] F. Bloch, “Über die Quantenmechanik der Elektronen in Kristallgittern”, *Zeitschrift für Physik* **52**, 555 (1929).
- [137] W. Heisenberg, “Zum Paulischen Ausschlussprinzip”, *Annalen der Physik* **402**, 888 (1931).
- [138] R. Peierls, “Elektronentheorie der Metalle”, *Ergebnisse der exakten Naturwissenschaften* **11**, 284 (1932).
- [139] J. E. Hirsch and F. Marsiglio, “Superconducting state in an oxygen hole metal”, *Phys. Rev. B* **39**, 11515-11525 (1989).
- [140] J.E. Hirsch, “Bond-charge repulsion and hole superconductivity”, *Physica C* **158**, 326 (1989).
- [141] J.E. Hirsch, “Coulomb attraction between Bloch electrons”, *Phys. Lett. A* **138**, 83 (1989).
- [142] J. E. Hirsch, “Why holes are not like electrons: A microscopic analysis of the differences between holes and electrons in condensed matter”, *Phys. Rev. B* **65**, 184502 (2002).
- [143] J. Hutchinson, M. Baker and F. Marsiglio, “The spectral decomposition of the helium atom two-electron configuration in terms of hydrogenic orbitals”, *Europ. J. of Phys.* **34**, 111 (2013).
- [144] J. E. Hirsch, “Inapplicability of the Hubbard model for the description of real strongly correlated electrons”, *Physica B* **199-200**, 366 (1994).
- [145] J. E. Hirsch, “Dynamic Hubbard Model”, *Phys. Rev. Lett.* **87**, 206402 (2001).
- [146] F. Marsiglio and J. E. Hirsch, “Hole Superconductivity and the High- T_c Oxides”, *Phys. Rev. B* **41**, 6435 (1990).
- [147] J. E. Hirsch, “Pairing of holes in a tight-binding model with repulsive Coulomb interactions”, *Phys. Rev. B* **43**, 11400 (1991).
- [148] F. Marsiglio and J.E. Hirsch, “Tunneling asymmetry: A test of superconductivity mechanisms”, *Physica C* **159**, 157 (1989).
- [149] J.E. Hirsch, “Thermoelectric power of superconductive tunnel junctions”, *Phys. Rev. Lett.* **72**, 558 (1994).
- [150] J.E. Hirsch, “Consequences of charge imbalance in superconductors within the theory of hole superconductivity”, *Phys. Lett. A* **281**, 44 (2001).
- [151] J.E. Hirsch, “Superconductors as giant atoms predicted by the theory of hole superconductivity”, *Phys. Lett. A* **309**, 457 (2003).
- [152] J. E. Hirsch, “Charge expulsion, charge inhomogeneity, and phase separation in dynamic Hubbard models”, *Phys. Rev. B* **87**, 184506 (2013).
- [153] J. E. Hirsch, “Dynamic Hubbard model: kinetic energy driven charge expulsion, charge inhomogeneity, hole superconductivity and Meissner effect”, *Phys. Scr.* **88**, 035704 (2013).
- [154] F. London, “Superfluids”, Vol. I, Dover, New York, 1961.
- [155] J.E. Hirsch, “Kinetic energy driven superconductivity, the origin of the Meissner effect, and the reductionist frontier”, *Int. J. Mod. Phys.* **25**, 1173 (2011).
- [156] J. E. Hirsch and F. Marsiglio, “London penetration depth in hole superconductivity”, *Phys. Rev. B* **45**, 4807 (1992).
- [157] F. London and H. London, “The electromagnetic equations of the supraconductor”, *Proc. Roy. Soc. A* **149**, 71 (1935).
- [158] F. London and H. London, “Supraleitung und diamagnetismus”, *Physica* **2**, 341 (1935).
- [159] J.E. Hirsch, “Charge expulsion and electric field in superconductors”, *Phys. Rev. B* **68**, 184502 (2003).
- [160] J. E. Hirsch, “Electrodynamics of superconductors”, *Phys. Rev. B* **69**, 214515 (2004).
- [161] J. E. Hirsch, “Predicted Electric Field near Small Superconducting Ellipsoids”, *Phys. Rev. Lett.* **92**, 016402 (2004).
- [162] J.E. Hirsch, “Spin Meissner effect in superconductors and the origin of the Meissner effect”, *Europhys. Lett.* **81**, 67003 (2008).
- [163] J.E. Hirsch, “Electrodynamics of spin currents in superconductors”, *Ann. Phys. (Berlin)* **17**, 380 (2008).
- [164] J. E. Hirsch, “The Bohr superconductor”, *Europhys. Lett.* **113**, 37001 (2016).
- [165] J. E. Hirsch, “The missing angular momentum of superconductors”, *J. Phys. Cond. Matt.* **20**, 235233 (2008).
- [166] P. A. Davidson, “An Introduction to Magnetohydrodynamics”, Cambridge University Press, Cambridge, 2001.
- [167] J. E. Hirsch, “Defying Inertia: How Rotating Superconductors Generate Magnetic Fields”, *Annalen der Physik* <https://doi.org/10.1002/andp.201900212> (2019).
- [168] J.E. Hirsch, “Materials and mechanisms of hole superconductivity”, *Physica C* **472**, 78 (2012) and references therein.
- [169] J. Kortus et al, “Superconductivity of Metallic Boron in MgB_2 ”, *Phys. Rev. Lett.* **86**, 4656 (2001).

- [170] S. Margadonna et al, “Pressure evolution of the low-temperature crystal structure and bonding of the superconductor FeSe ($T_c = 37\text{K}$)”, [Phys. Rev. B 80, 064506 \(2009\)](#).
- [171] J. E. Hirsch, “Effect of orbital relaxation on the band structure of cuprate superconductors and implications for the superconductivity mechanism”, [Phys. Rev. B 90, 184515 \(2014\)](#).
- [172] A.P. Drozdov, M. I. Erements and I. A. Troyan, “Conventional superconductivity at 190 K at high pressures”, [arXiv:1412.0460 \(2014\)](#).
- [173] J.E. Hirsch and F. Marsiglio, “Hole superconductivity in H_2S and other sulfides under high pressure”, [Physica C 511, 45 \(2015\)](#).
- [174] Winston Churchill’s speech to the House of Commons, [November 10, 1942](#).
- [175] T. Wang et al, “Absence of conventional room-temperature superconductivity at high pressure in carbon-doped H_3S ”, [Phys. Rev. B 104, 064510 \(2021\)](#).
- [176] K. R. Popper, “The Logic of Scientific Discovery”, Routledge Classics, London, 1959.
- [177] J. E. Hirsch, “Superconductivity begins with H”, [World Scientific, Singapore, 2020](#). btem
- [178] V. S. Minkov et al, “The Meissner effect in high-temperature hydrogen-rich superconductors under high pressure”, [DOI:10.21203/rs.3.rs-936317/v1](#) (October 4, 2021).
- [179] J. E. Hirsch and F. Marsiglio, “Clear evidence against superconductivity in hydrides under high pressure”, [arXiv:2110.07568 \(2021\)](#).